

# UCSF

## UC San Francisco Previously Published Works

### Title

The Northwest Geysers EGS Demonstration Project, California Part 1: Characterization and reservoir response to injection

### Permalink

<https://escholarship.org/uc/item/9fw929zm>

### Authors

Garcia, Julio  
Hartline, Craig  
Walters, Mark  
[et al.](#)

### Publication Date

2016-09-01

### DOI

10.1016/j.geothermics.2015.08.003

Peer reviewed

1  
2  
3  
4  
5  
6  
7  
8  
9  
10  
11  
12  
13  
14  
15  
16  
17  
18  
19  
20  
21  
22  
23  
24  
25  
26  
27  
28  
29  
30  
31  
32

***The Northwest Geysers EGS Demonstrations Project, California  
Part 1: Characterization and Reservoir Response to Injection***

Julio Garcia<sup>1\*</sup>, Craig Hartline<sup>1</sup>, Mark Walters<sup>1</sup>, Melinda Wright<sup>1</sup>, Jonny Rutqvist<sup>2</sup>, Patrick F. Dobson<sup>2</sup>, and Pierre Jeanne<sup>2</sup>

<sup>1</sup> Calpine Corporation, Middletown, CA 95461, U.S.A.

<sup>2</sup> Lawrence Berkeley National Laboratory (LBNL), Berkeley, CA 94720 U.S.A.

\* Corresponding author. Tel.: +1-707-631-6068, fax.: +1-707-431-6148  
E-mail address: [julio.garcia@calpine.com](mailto:julio.garcia@calpine.com) (J. Garcia)

For EGS special issue Geothermics

This is author’s final version that was published as:

Garcia, J., Hartline, C., Walters, M., Wright, M., **Rutqvist, J.**, Dobson, P.F., Jeanne, P. The Northwest Geysers EGS Demonstration Project, California - Part 1: Characterization and reservoir response to injection. *Geothermics*, **63**, 97–119 (2016)

**34ABSTRACT**

35An Enhanced Geothermal System (EGS) Demonstration Project is currently underway in the  
36Northwest Geysers. The project goal is to demonstrate the feasibility of stimulating a deep high-  
37temperature reservoir (HTR) (up to 400°C, 750°F). Two previously abandoned wells, Prati State 31  
38(PS-31) and Prati 32 (P-32), were reopened and deepened to be used as an injection and production  
39doublet to stimulate the HTR. The deepened portions of both wells have conductive temperature  
40gradients of 10°F/100ft (182°C/km), produce connate native fluids and magmatic gas, and the rocks  
41were isotopically unexchanged by meteoric water. The ambient temperature meteoric water injected  
42into these hot dry rocks has evidently created a permeability volume of several cubic kilometers as  
43determined by seismic monitoring. Preliminary isotopic analyses of the injected and produced water  
44indicate that 50% to 75% of the steam from the created EGS reservoir is injection-derived.

45

46

47

## 481 INTRODUCTION

49The Geysers Geothermal field is the world's largest geothermal electricity generating operation and  
50has been in commercial operation since 1960. It is a vapor-dominated geothermal reservoir system that  
51was developed to a maximum installed capacity of 2043 MWe by 1987. Subsequently, a number of  
52peripheral developed areas were abandoned because of resource problems including declining steam  
53pressure, low permeability, corrosive steam and high non-condensable gas (NCG) concentrations. As a  
54result of the high steam withdrawal rates, the reservoir pressure declined until the mid 1990s, when  
55increasing injection rates resulted in a stabilization of the steam production and reservoir pressure. In  
56recent decades operators have been relying heavily on supplemental water injection to sustain its  
57current generation of 825 MWe.

58The concept of Enhanced Geothermal Systems (EGS) at The Geysers differs from other EGS  
59programs pursued elsewhere in the world. At The Geysers, EGS projects target areas which contain a  
60significant portion of the recoverable geothermal energy in the system that is currently underutilized.  
61The main focus is on the revival of production from peripheral areas by using water injection to  
62increase reservoir pressure, increase permeability, reduce NCG concentrations and mitigate corrosion.  
63Although this scope is somewhat site-specific, the vast unexploited heat resource and existing  
64infrastructure at The Geysers offers an opportunity for significant short-term EGS generation.

65The EGS Demonstration Project is in the northwestern portion of The Geysers geothermal field  
66(Figure 1) where a high temperature reservoir (HTR) with temperatures up to 400°C (750°F) was  
67previously identified ([Walters et al., 1992](#) and [Walters and Beall, 2002](#)). The HTR underlies a normal  
68temperature reservoir (NTR) where temperatures are about 240°C (465°F).

69The EGS Demonstration Project area was originally explored in the 1980s with three exploration and  
70development wells in the Central California Power Agency (CCPA) steam field. These wells were  
71never produced due to high concentrations of NCG produced from the HTR and were abandoned in  
721999 after the CCPA #1 Power Plant was closed for economic reasons and later decommissioned.

73Two of the previously abandoned wells, Prati State 31 (PS-31) and Prati 32 (P-32), were reopened,  
74deepened and re-completed in 2010 for direct injection and stimulation of the HTR. The NTR in the  
75project area is relatively shallow (the base of the NTR is at an elevation of -1800 m mean sea level (m-  
76msl), -6000 feet (ft-msl)) and the project wells are sufficiently deep to penetrate the upper portion of  
77the HTR (Figure1).

78The intent of the EGS Demonstration Project is to show that the permeability of the HTR can be  
79stimulated by fracture reactivation to create a diffuse “cloud” of fractures rather than a localized  
80fracture plane when relatively cool water is injected into a very hot rock volume at low flow rates (65  
81l/s) and low pressures (< 10 MPa). Water injection into the HTR was anticipated to lower the  
82concentrations of NCG as well as to provide a sustainable steam supply for nearby steam production  
83wells. Initiation of this project was also motivated by evidence for an inadvertently created EGS at  
84depths of 3 to 5 km in the HTR about 3 miles southeast of the EGS Demonstration project area ([Stark,](#)  
852003).

86To date, the data shows a strong and favorable reservoir response to the injection, including increases  
87in pressure and flowrate at nearby production wells, and order-of-magnitude decreases in non-  
88condensable gas content of the produced steam. The area stimulated is evidently partially isolated from  
89the main reservoir to the SE, based on data from wellhead pressures, microearthquake monitoring,  
90noncondensable gas concentrations and rock isotope values. The isolation appears to be controlled by a  
91previously-mapped NE-trending fault zone. The EGS injection experiment was not successful in  
92mitigating the corrosive effects of chloride-bearing steam, which resulted in corroded casing of the  
93production well, PS-31.

94The Northwest Geysers EGS Demonstration Project is a collaborative effort between scientists and  
95engineers at Calpine and Lawrence Berkeley National Laboratory (LBNL) and is funded by the US  
96Department of Energy's (DOE) Geothermal Technologies Office and Geysers Power Company  
97(Calpine). The project is organized into three phases:

98Phase I: Pre-stimulation. During Phase I, initiated in 2009, a stimulation plan was developed based on  
99a detailed geological model, analysis of historical data, and pre-stimulation modeling ([Garcia et al.,  
1002012](#)). 3-D realizations of the main geologic units together with the incorporation of rock properties  
101from previous unpublished core studies (density, permeability, porosity, and rock strength) constituted  
102the input data for the geologic model created near PS-31 and P-32. A set of stimulation scenarios were  
103presented by [Rutqvist et al. \(2010\)](#) and [Rutqvist et al. \(2015b\)](#) from a coupled thermal, hydraulic, and  
104mechanical (THM) model developed at LBNL.

105Phase II: Reservoir Stimulation. This phase commenced in October 2011 with injection of tertiary  
106treated wastewater from the Santa Rosa Geysers Recharge Project (SRGRP) into the HTR via P-32  
107([Garcia et al, 2012](#)). It is important to note that the injection into P-32, as well as all injection at The  
108Geysers, is not pumped and falls from the wellhead under a vacuum of about -0.7 to -0.9 bars (-10 to  
109-13 psig).

110Phase III: Long Term Data Collection, Monitoring, and Reporting. This phase will recommence in  
1112016.

112This paper summarizes Phase I field work including wellbore readiness and baseline testing, along  
113with Phase II results including analysis of the reservoir's response to stimulation by injection. An  
114accompanying paper titled, "The Northwest Geysers EGS Demonstration Project, California - Part 2:  
115Modeling and Interpretation" presents the results of coupled thermal, hydraulic, and mechanical  
116(THM) modeling ([Rutqvist et al., 2015a, this issue](#)).

117

## 1182 **GEOLOGICAL AND GEOTHERMAL SETTING**

119

### 1202.1 **Regional Geology**

121

122Structurally, The Geysers geothermal reservoir is within the terrane of the San Andreas Fault system  
123(Figure 1), and is influenced by Mesozoic subduction, Tertiary thrust faulting, and high-angle  
124Quaternary faults. The relative motion between the Pacific Plate and North American Plate has been

125accommodated by right-lateral strike-slip motion along the San Andreas Fault Zone (DeCourten,  
1262008). The slip rates within this zone of subparallel, right-lateral, strike-slip faults progressively  
127decrease to the east and created a transtensional tectonic environment between the active Maacama  
128Fault Zone and the active Bartlett Springs Fault Zone. The modern-day Geysers geothermal field is  
129bounded to the southwest by the inactive Big Sulphur Creek – Mercuryville Fault Zone, and to the  
130northeast, by the inactive Collayomi Fault Zone. There are no faults in or adjacent to The Geysers  
131which are known to be active within the last 15,000 years.

132Oppenheimer (1986) indicated that seismic sources in The Geysers occur from what appear to be  
133almost randomly-oriented fracture planes. Lockner et al. (1982) performed experiments to determine  
134the mechanical characteristics of rocks from the reservoir at The Geysers. They concluded that  
135fracturing and hydrothermal alteration had weakened the rock sufficiently such that the reservoir rock  
136is only able to support a frictional load.

137Within The Geysers the maximum horizontal principal stress is oriented about N26E (Boyle and  
138Zoback, 2014). They used a large set of earthquake focal mechanisms recorded in the Northwest  
139Geysers during the period of January 2005 - May 2012 to determine stress orientations. They  
140concluded that in the Northwest Geysers, fractures appeared to have a N60E direction of strike in the  
141fractured metagraywacke interval comprising the main reservoir, and a bimodal distribution of  
142fractures in the deepest reservoir where the two sets of predominant fractures are N30E and N85E.  
143The corresponding intermediate principal stress is approximately equal in magnitude to the maximum  
144horizontal principal stress and has a vertical orientation.

145

## 1462.2 Local Geology

147

148The EGS Demonstration project area is part of an undeveloped, 10 square-mile portion of the  
149northwest Geysers geothermal field between the Aidlin Power Plant (Calpine Unit 1) and the

150Ridgeline Power Plant (Calpine Units 7 and 8). In the project area, the HTR is at its shallowest depth  
151(2440 m, 8000 ft) and has been identified from pressure-temperature logs to be at elevations of -1680  
152to -1830 m-msl (-5500 to -6000 ft-msl) (Figure 1).

153Figure 2 is a geologic map showing detailed surface geologic mapping and Quaternary faults in the  
154northwest Geysers. The surface geology of the EGS Demonstration area is part of the Franciscan  
155Assemblage (200 to 80 Ma in age) and mapped in Figure 2 as a greenstone complex (fgs), a relative  
156shallow mélange dominated by metagraywacke and argillite with minor amounts of greenstone and  
157traces of blueschist (fsrgw), and turbidite sequences of metagraywacke and argillite (fgw). Six  
158Quaternary surface faults mapped on the basis of lithologic discontinuities and geomorphic lineaments  
159appear to extend to reservoir depth and divide the northwest Geysers reservoir into compartments  
160separated by hydraulic discontinuities. These are the Mercuryville, Alder Creek, Squaw Creek,  
161Ridgeline, Caldwell Pines and Caldwell Ranch faults which are labeled in Figure 2.

162The cross section through the EGS Demonstration area in Figure 3 shows that greenstone and  
163metagraywacke form the caprock over the metagraywacke reservoir. Consequently metagraywacke  
164forms both the caprock and reservoir in the EGS project area; the only difference is that the reservoir  
165metagraywacke is fractured rock through which hydrothermal fluids have passed and the cap rock  
166metagraywacke is not fractured and not hydrothermally altered.

167During the course of the EGS Demonstration, a short (4.8 km), northeast-trending fault delineated by  
168detailed surface mapping (by Walters, M., 1985-1990, in: [Nielson et al.,1991](#), and labeled Caldwell  
169Pines Fault in Figure 2) was determined to extend from the surface into the reservoir. This short fault  
170or shear zone appears to create a hydraulic discontinuity (or leaky barrier) between the EGS  
171Demonstration wells and the Caldwell Ranch Project wells (e.g. Prati 38) to the south with a  
172differential reservoir pressure of up to  $6.2 \times 10^5$  Pa (90 psig) on either side of the fault.

173



### 1742.3 Reservoir Geology

175The geothermal resource in the EGS area was explored by PS-31 and P-32, and the nearby steam  
176production wells Prati 25, Prati 37 and Prati 38 (Walters et al., 1992). The HTR in P-32 was  
177encountered near a measured depth of about 2.6 km (8400 ft - referenced to ground surface). Flowing  
178steam temperatures at the bottom of the P-32 well were logged at 347°C (656°F) (Walters et al.,  
1791992). Where pressure-temperature-spinners (PTS) logs were available, the calculated enthalpies in  
180the northwest Geysers HTR ranged from 3020 kJ/kg to 3070 kJ/kg (1,300 to 1,320 BTU/lb) with an  
181apparent temperature gradient ranging from approximately 15 to 30°C /100m (5 to 10°F /100ft)  
182(Walters et al., 1992).

183The six Quaternary faults which form hydraulic discontinuities and compartmentalize the northwest  
184Geysers reservoir also appear to delineate isotopically different reservoir blocks: some reservoir rock  
185volumes are isotopically less-exchanged by meteoric water rather than the isotopically more-  
186exchanged rocks typically found throughout the reservoir at The Geysers. All of the isotopic analyses  
187for the EGS Demonstration Project are presented in the delta notation,  $\delta$ ; as parts per thousand (per  
188mil, or ‰) deviation of isotopic ratios  $^{18}\text{O}/^{16}\text{O}$  or D/H, relative to Standard Mean Ocean Water  
189(SMOW). Whole-rock, metagraywacke  $\delta^{18}\text{O}$  values decrease from +12 per mil at the top of the NTR  
190to +4 of the Geysers reservoir (Moore and Gunderson, 1995 and Walters et al., 1996). Walters and  
191Beall (2002), respectively, confirmed this same relationship of decreasing whole-rock metagraywacke  
192 $\delta^{18}\text{O}$  values with depth in the High Valley area to the east, and the Aidlin area to the west of the EGS  
193Demonstration Area. However, in the EGS Demonstration area, the metagraywacke in the NTR is only  
194weakly exchanged by meteoric water, and new metagraywacke  $\delta^{18}\text{O}$  values from the deepened PS-31  
195and P-32 wells are evidence the HTR is apparently not exchanged by meteoric water. That is, the  
196metagraywacke  $\delta^{18}\text{O}$  values in both the caprock and HTR in the EGS Demonstration area are in the  
197same range (+12.0 per mil). Taken together with the conductive temperature gradients, the

198unexchanged whole-rock metagraywacke  $\delta^{18}\text{O}$  values are evidence that the created EGS reservoir is in  
199non-hydrothermal, hot “dry” rock.

200Figure 4 graphically compares the whole-rock isotopic profiles of metagraywacke  $\delta^{18}\text{O}$  values typical  
201of Northwest Geysers wells to wells located in the EGS area and Caldwell Ranch project area. Figures  
2025 and 6 present these data as geologic cross-sections. North of the Caldwell Ranch Fault and Caldwell  
203Pines Fault, the NTR rock in the EGS Demonstration area is only weakly exchanged with meteoric  
204water, and the HTR rock is unexchanged (Figure 5). Here the reservoir rock in the EGS are  
205unexchanged with meteoric water and are in the same range as the caprock compared to the typical  
206Geysers reservoir.

207Many early (1977-1985)  $\delta^{18}\text{O}$  values in the steam condensate throughout the Northwest Geysers,  
208including the EGS project, ranged from 0 per mil to +3 per mil (Figure 7). Positive  $\delta^{18}\text{O}$  values  
209indicate that the native steam in this area was not significantly influenced by meteoric water and may  
210be connate water ([Lutz et al., 2012](#)) (see Section 5.3.1).

211Pressure data, reservoir modeling, isotopic and NCG data, as well as published analysis of temperature  
212logging by the U.S. Geological Survey indicates that the EGS Demonstration Area is younger and  
213partially isolated from the NTR steam reservoir to the south, east and west. Steam from the HTR  
214contains much higher NCG concentrations and higher pressures than the depleted NTR steam fields to  
215the southeast of the EGS project. The high temperatures recorded in the HTR suggests to us that the  
216project area is underlain by a recent granitic intrusion (Figure 3), which is estimated to have begun  
217cooling 5,000 to 10,000 years before the present ([Williams et al., 1993](#)).

218

## 2193 **PHASE I: PRE-STIMULATION**

220

### 2213.1 **Wellbore Readiness**

222

223Two previously abandoned wells, PS-31 and P-32, were reopened and deepened as an EGS  
224production-injection well pair, respectively, in the HTR. Well testing indicated there is some localized  
225permeability in the HTR as evidenced by steam entries in the HTR in both wells (Figure 8).

226

227

228

### 229**3.1.1 Recompletion of Wells**

230

231The EGS Demonstration Project was initially planned for PS-31 and P-32 to comprise an injection and  
232production well pair, respectively. However, after deepening these wells, a significant steam entry was  
233identified at 3352 m (11,000 ft) in P-32 with a temperature of 400°C (750°F) (Figure 8 and 9). The  
234high temperature and apparent permeability in P-32 resulted in a revised plan to use P-32 as the  
235injection well and PS-31 as the production well.

236Figure 9 shows good agreement between the temperature profiles from P-25 and PS-31. These  
237pressure-temperature (PT) surveys confirmed the temperature of the NTR at around 232°C (450°F)  
238and the underlying HTR indicative of a conductive temperature gradient (10°F/100ft depth increase,  
239or 18.2°C/100m) with a maximum temperature of about 400°C (750°F) near the bottom of the well  
240at 3352 m (11000 ft) measured depth.

241Conductive high temperature systems underlying typical vapor-dominated reservoirs were previously  
242reported at The Geysers by [Drenick \(1986\)](#), [Walters et al. \(1988\)](#), and [Nielson and Moore \(2000\)](#). At  
243the Larderello-Travale geothermal field, a hydrothermal system similar to The Geysers, the presence  
244of a deep convective high temperature reservoir was originally published by [Bertini in 1985](#). For  
245additional information on the origin of the HTR at The Geysers the reader is referred to [Truesdell](#)  
246[\(1991\)](#) and [Beall and Wright \(2010\)](#). The effect of injection and the complex fluid and heat flow  
247processes in HTR have been studied using numerical simulations by [Pruess et al. \(1987\)](#), [Truesdell](#)  
248[and Shook \(1997\)](#), [Shook \(1993\)](#) and [Pruess et al. \(2007\)](#). Both [Pruess et al. \(2007\)](#) and [Truesdell and](#)

249 Shook (1997) showed that injection into the HTR has a favorable effect in terms of a reduction of  
250 NCG content. Such reduction on NCG content due to injection has been observed throughout The  
251 Geysers and also at the EGS site.

252 The well designs were modified to accommodate the decision to switch P-32 to injection and PS-31 to  
253 production: (1) P-32 was deepened from 2926 m (9600 ft) to 3396 m (11143 ft) and a 5-1/2" (inch=")  
254 blank liner was hung from the surface to 2590 m (8500 ft) (Figure 10). Below 2590 m (8500 ft) depth,  
255 the well was not modified and a slotted liner was installed from 2590 m (8500 ft) to 3398 m (11115 ft)  
256 where water is injected at a rate of about 44.2 kg/s (700 gpm) into the HTR. (2) Initially, PS-31 was  
257 deepened from 2743 m (9000 ft) to 3058 m (10034 ft) in August 2010 with about 610 m (2000 ft) of  
258 slotted liner installed within the HTR. To switch PS-31 over to a production design, the upper portion  
259 of the lower blank liner was perforated, allowing the well to communicate with both the NTR and the  
260 HTR (Figure 10).

261 The deepening of the EGS production-injection well pair into the HTR was significantly affected by  
262 the high rock temperatures which slowed the rate of penetration while air drilling from a typical rate of  
263 5 to 6 m/h (15 to 20 ft/h) to less than 3 m/h (10 ft/h). Figure 11 shows the bit condition after 30.5 m  
264 (100 ft) of air drilling P-32 to final depth of 3396 m (11143 ft).

265

### 266 3.1.2 Well and Reservoir Testing

267

268 Before recompletion of P-32 as an injector, it was flow tested with a resulting steam flow rate of 10.6  
269 kg/s ( $84.4 \times 10^3$  lb/h (or kph)) at a normalized pressure of  $6.9 \times 10^5$  Pa (100 psig), 4.5 wt% NCG  
270 concentration with 1,322 ppmw H<sub>2</sub>S, and chloride concentration in the steam condensate of 47 ppmw.  
271 Sharp pressure drops at PS-31 (step changes of approximately 3 psi) during flow testing of P-32,  
272 provided early evidence of the degree of connectivity between these two wells (Figure 12).

273 Three well testing campaigns were made in PS-31, and the corresponding PTS logging results are  
274 graphed in Figure 13. The first test was completed on October 13, 2010 before PS-31 was recompleted

275as a producer. Thus, the 3-day isochronal flow test was completed with the NTR behind unperforated  
276liner. A flow rate of 5.4 kg/s (42.9 kph) at a normalized pressure of  $6.9 \times 10^5$  Pa (100 psig) with a  
277wellhead enthalpy of 2761 kJ/kg (1188 BTU/lb) was observed (well head temperature - WHT =  $160^\circ\text{C}$   
278( $321^\circ\text{F}$ ), and well head pressure -WHP =  $4.6 \times 10^5$  Pa (67 psig)). The maximum shut-in WHP following  
279the well test was 323 psig. Pressure transient data following the flow test were used to estimate near-  
280well reservoir permeability. Pressure build-up analysis results provided an estimated value of 22,000  
281md-ft (6.7 Dm) for fracture transmissivity (kh). The kh at The Geysers ranges from 5,000 md-ft to  
282400,000 md-ft (values based on prior pressure transient analysis performed at The Geysers and from  
283values obtained for the reservoir model). Assuming a 2,000 ft-thick production interval (Figure 10) at  
284PS-31, the resulting permeability is 10 md ( $1 \times 10^{-14}$  m<sup>2</sup>). The low permeability estimated during the  
285flow test of October 13, 2010 is comparable to values encountered at other wells in the Northwest  
286Geysers. The total NCG concentration in the steam was 4.5 wt% with 1386 ppmw H<sub>2</sub>S and 135 ppmw  
287chloride concentration in the steam condensate. The PTS log made during this flow test showed  
288superheated steam flowing up the well bore to about 365 m (1200 ft) depth and saturated steam from  
289about 365 m (1200 ft) to the surface. After the perforations were shot in the 7" blank liner from 2065  
290m to 2346 m (6776 ft to 7696 ft), PS-31 was tested a second time on September 6-7, 2011. PS-31  
291flowed 6.64 kg/s (52.7 kph) at a normalized pressure of  $6.9 \times 10^5$  (100 psig). The increased flow rate  
292was attributed to steam entries from the NTR where the blank liner had been perforated. A third flow  
293test of PS-31 was made on September 28, 2011. The flow rate from PS-31 measured during this test  
294was the same as the September 6, 2011 flow rate. A difference in the pre-perforation PTS logs versus  
295post-perforating logs is that the spinner shows an increase of about 1,000 rpm above the top  
296perforation (2065 m - 6776 ft). This is a consequence of an increased flow rate of 1.26 kg/s (10 kph)  
297from nine steam entries in the NTR which were covered with 7 inch blank liner section prior to the  
298perforation job between 2065 m to 2346 m (6776 ft to 7696 ft).

299

## 3004 PHASE II: RESERVOIR STIMULATION

301

302 Injection into P-32 began on October 6, 2011 at 10:20 am. In accord with the typical injection startup  
303 procedure for new injection wells at The Geysers, the well received a high initial injection rate of 70-  
304 76 kg/s (1100-1200 gpm). The high rate was continued for 12 hours then reduced to approximately  
305 25.3 kg/s (400 gpm) and was maintained for 55 days. Figure 14 shows the early injection history into  
306 P-32 and WHP increases in the three closer and shut-in wells, PS-31, Prati 38 (P-38) and P-25. As with  
307 all other injection wells in The Geysers steam field, water is injected into P-32 under gravity (not by  
308 pumping) causing the steam in the well bore and nearby formation to collapse which draws the water  
309 into the wellbore and surrounding rock under a vacuum. The measured vacuum at the wellhead in  
310 Geysers injection wells ranges from -0.7 to -0.9 bars (-10 to -13 psig).

311 Figure 14 shows that pressure response to P-32 injection at PS-31 and P-25 is greater than at P-38. It is  
312 also important to note that injection into P-32 had a stronger effect on PS-31 than P-25 although the  
313 separation distances at the total depths of these wells between P-32 and PS-31, and P-32 and P-25, are  
314 similar, 525 m (1723 ft) and 463 m (1519 ft), respectively. It is also possible that the influence of P-32  
315 injection might have been felt at depths less than total depth (TD), where PS-31 is closer to P-32.

316 Since P-32 injection began, five injectivity tests have been conducted (October 17, 2011; November  
317 15, 2011; January 11, 2012; March 6, 2012 and June 18, 2012). Figure 15 shows the pressure,  
318 temperature, injection rate and tool depth plotted versus time during the step-rate injectivity test of  
319 November 15, 2011. During this test, the tools were traversed to 2195 m (7200 ft) at approximately 46  
320 m/min (150 ft/min) while injecting water at approximately 13.6 kg/s (215 gpm). The tools were then  
321 held at 2195 m (7200 ft) depth for 15 minutes. Then the tools traversed to the test depth of 3338 m  
322 (10950 ft) at 15 m/min (50 ft/min) while injecting at 39 kg/s (600 gpm). Once at 3338 m (10950 ft),  
323 the injection was maintained for approximately one hour at each injection step at rates of 39 kg/s (600  
324 gpm), 56.9 kg/s (900 gpm) and 76 kg/s (1200 gpm).

325 The water levels (depths measured from the surface) versus injection rates for the first two tests on

326 October 17, 2011 and November 15, 2011 are shown in Figure 16. These two injectivity tests indicated  
327 that the water level had little sensitivity to injection rate and that apparently injectivity did not improve  
328 from October 17, 2011 to November 15, 2011. One possibility is that the nature of the step injectivity  
329 tests do not capture the transient behavior of injection as possible a “falling head” (water column)  
330 injectivity test will be accomplished. In order to increase stimulation of the deepest entry in the HTR and  
331 to increase the overall injectivity at P-32, the injection rate was increased from 25.3 kg/s (400 gpm) to  
332 65.1 kg/s (1000 gpm) on November 30, 2011.

333 Figure 17 summarizes the effect of injection at P-32 on wells PS-31 and P-25. Early results of the  
334 stimulation phase show injection into P-32 caused substantial pressure increases in the reservoir  
335 pressure as measured at the PS-31 well head, from  $22.3 \times 10^5$  Pa to  $29.5 \times 10^5$  (323 to 428 psig), and  
336 from  $23.8 \times 10^5$  to  $25.3 \times 10^5$  (345 to 367 psig) at P-25 during the first injection step of 25.3 kg/s (400  
337 gpm) which lasted 43 days. The injection in P-32 resulted in an increased flow rate at P-25 of 1.6 kg/s  
338 (13 kph) of superheated steam. When tested on May 17, 2010, a flow rate of 8.1 kg/s at  $7.6 \times 10^5$  (64  
339 kph at 110 psig) was measured at the P-25 wellhead. By January 20, 2012, P-25 was flowing 9.7 kg/s  
340 (77 kph) at  $7.44 \times 10^5$  108 psig WHP. After the water injection rate was raised from 25.3 kg/s (400 gpm)  
341 to 65.1 kg/s (1000 gpm) on November 30, 2011, the rate of the static WHP increases at PS-31 and P-  
342 25 accelerated. The maximum WHP recorded at PS-31 was  $32.0 \times 10^5$  (465 psig). This represents an  
343 increase of  $9.7 \times 10^5$  (140 psig) from pre-stimulation values. It is apparent from Figure 17 that the rate  
344 of pressure increase at PS-31 declined after P-25 was put into production on December 09, 2011. In  
345 addition to steam production at P-25, reductions of injection rates at P-32 contributed to a decline of  
346 static wellhead pressures at PS-31. Figure 17 shows a stair step in the WHP curve at PS-31 on January,  
347 2012. This step coincides with wireline activity (Static PT followed by a flow test) and can be  
348 explained as follows. When shut-in, P-31 tends to gas-up at the top of the wellbore (steam circulating  
349 inside and releasing CO<sub>2</sub> at the top). Under static conditions, what is recorded at the surface is the  
350 reservoir pressure minus (-) the “weight” of the steam+gas inside the wellbore. During the static PT

351some gas escaped from the wellhead lubricator and evidently the rest of the gas cap was released  
352during the flow test. Calculation of the pressure profile inside the well based on the static PT confirms  
353the assumption that the well was indeed capped by CO<sub>2</sub> resulting in a different well head pressure as if  
354the wellbore were only filled with saturated steam.

355During the injection stimulation phase, two flow tests were conducted at PS-31 on January 31, 2012  
356and June 14, 2012 with resulting flow rates of 9.1 kg/s and 11.8 kg/s (72 kph and 94 kph) respectively.  
357The increase in flow is primarily attributed to the removal of the PS-31 upper liner (Figure 12) as the  
358well was finally converted from an injector to a producer on April 4, 2012. A pressure transient  
359analysis following the flow test of June 14, 2012 indicated that the kh increased to 12.69 Dm (42300  
360md-ft) from the 6.6 Dm (22000 md-ft) value found when the well was re-opened. This increase is  
361considered small. Nevertheless, it is an indication that permeability has increased at the EGS site,  
362albeit at a low rate.

363 Following the stimulation injection phase, water injection at P-32 was suspended for a period of 160  
364days. The wellhead pressure at PS-31 decreased rapidly indicating again that both wells are extremely  
365well connected. PS-31 began steam production on December 5, 2012 which continued until February  
36613, 2013 when near-surface corrosion of the well casing caused a steam leak. This leak necessitated  
367shutting-in the well. PS-31 will remain shut-in until a corrosion-resistant high alloy or titanium tie-  
368back liner is installed to prevent future corrosion.

369

## 3705 **MONITORING**

371

### 3725.1 **Microseismic monitoring**

373  
374A permanent Lawrence Berkeley National Laboratory (LBNL) seismic monitoring network has  
375operated since October 2003 and currently consists of 32 digitally-telemetered, three-component  
376seismic stations located within and slightly beyond The Geysers production boundaries. The recorded  
377seismic events are transmitted via radio telemetry to an on-site LBNL server, processed in real-time



378and integrated into the Northern California Seismic Network (NCSN). The NCSN is part of a much  
379larger and less densely sampled network operated by the United States Geological Survey (USGS).  
380Calpine's Geysers seismicity analysis generally utilizes this integrated online LBNL/USGS dataset  
381which is archived hourly at the University of California Berkeley's Northern California Earthquake  
382Data Center (NCEDC). For detailed analysis of the Northwest Geysers EGS Demonstration Project,  
383microseismicity data are acquired directly from a dedicated LBNL database. The seismic databases  
384noted above are available to the public online (Figure 18).

385Two temporary LBNL three-component seismic monitoring networks were also installed in separate  
386campaigns to monitor the EGS Demonstration Project area. In 2010, five stations were uniformly  
387distributed within about one mile of P-32. In 2011, sixteen stations were installed as a focused array to  
388collect specific data during the start-up of the EGS stimulation. Data from these temporary stations  
389have been downloaded and analyzed in detail at regular intervals. This temporary station data has been  
390processed independently by LBNL experts and also merged with the permanent LBNL station data to  
391provide a dense spatial sampling of the EGS demonstration project area.

392Calpine has completed detailed seismicity analysis using the dedicated LBNL database associated with  
393the EGS Demonstration at regular intervals for a volume surrounding the P-32 injection well. The time  
394range for seismicity analysis within this study (unless otherwise noted) is 01 September 2011 through  
39505 March 2013, primarily due to early 2013 complications with PS-31 well casing corrosion. During  
396the seismicity analysis time range, seven seismic events associated with the EGS Demonstration  
397Project exceeded M 2.50, the largest being a M 2.87 on 31 May 2012 (Figure 19). The energy release  
398of a seismic event is determined by the shear modulus (rigidity), the area of rupture and the slip rate  
399(Hanks and Kanamori, 1979; Aki and Richards, 1980; Segall, 1998). The SW to NE alignment of six  
400of the seven  $M \geq 2.50$  seismic events along the southeast boundary of the EGS seismicity cluster is  
401believed to represent a fracture zone with slightly increased surface areas. An eighth  $M \geq 2.50$  seismic  
402event of magnitude 3.74 occurred after the detailed seismicity analysis period on 21 January 2014.

403A near absence of seismicity was observed within the EGS Demonstration area in the 40 days prior to  
404the start of injection in P-32, with only one event of magnitude 0.63 recorded (see Figure 20). The 06  
405October 2011 onset of injection and steady 400 gpm flow rates produced an anticipated occurrence of  
406low-magnitude seismicity in the vicinity of P-32. The 29 November 2011 transition from 400 gpm to  
4071,000 gpm flow rates then resulted in a significant increase in microseismic event frequency (from  
408approximately 8 events per day to 42 events per day) followed by a gradual decline in frequency  
409toward previous levels (Figure 20 and 21). In general, the frequency of microseismic events initially  
410increased with an injection flow rate increase and then declined over time. The frequency of seismic  
411events declined significantly almost immediately after an injection flow rate decrease, and returned to  
412nearly background seismicity levels after approximately 80 days at 0 gpm (Figures 20 and 21).

413The majority of early seismicity after injection began was relatively near the injection center of P-32.  
414Significantly more events occurred to the north and northwest with increasing time, including several  
415time-limited and volume-limited clusters or linear alignments that appear to indicate fracture  
416reactivation within a previously unaffected volume. Seismic event hypocenter development viewed in  
4173D time animations suggests preferential water movement along NNW/SSE trending, steeply-dipping  
418zones of higher permeability (Figure 22).

419The average hypocenter descended by approximately 3.6 feet per day during approximately 520 days  
420of data analysis (including days 320 to 480 without injection). The rate of descent was highly  
421dependent on injection flow rate, with a maximum descent rate of 14.5 feet per day during the 98 day  
422period of sustained 1,000 gpm injection. A descent rate of 2.7 feet per day then occurred during the  
423subsequent 103 day period of sustained 700 gpm injection (Figure 23). After 270 days of P-32  
424injection, a time vs. subsea depth graph prepared using the LBNL microseismicity data suggested an  
425apparent deepening of the average hypocenter position within the EGS Demonstration Project area  
426that existed for approximately 18 days. Additional investigations indicated that this phenomenon  
427occurred for the LBNL microseismicity data throughout its Northwest Geysers coverage area. There is  
428no evidence that this is an artifact resulting from a variation in the seismic event processing

429 algorithms. However, this apparent deepening seems to be very much subdued to absent for archived  
430 Northern California Earthquake Data Center (NCEDC) data. It is possible that the apparent deepening  
431 seen on the more highly resolved LBNL microseismicity data may be attributed to reactivation of  
432 deeper structures associated with regional tectonics. However, due to concerns with data reliability, no  
433 conclusions have been drawn based on data associated with this apparent deepening.

434 The apparent SW to NE  $M \geq 2.50$  seismicity alignment seen to the southeast of P-32 is consistent with  
435 a previously mapped northeast-trending surface zone of faulting (Nielson et al., 1991) and a known  
436 reservoir pressure boundary (Figure 24). The timing of these  $M \geq 2.50$  seismic events does not show a  
437 particularly strong correlation with injection rate or injection rate variability (Figures 17 and 20).

438 A very positive outcome of the EGS Demonstration Project in terms of induced seismicity analysis is  
439 an improved understanding of the relationship between Geysers induced seismicity patterns and  
440 apparent fluid flow paths and fluid boundaries. The detailed seismicity investigations conducted in  
441 association with this project by Calpine Corporation and those completed in collaboration with LBNL  
442 (e.g. Jeanne et al. 2014b and Rutqvist et al. (2015a), this issue) all indicate linear alignment of  
443 seismicity hypocenters (representing hydraulic discontinuities) that correlate very well with other  
444 constraints such as lithology logs, well pressure measurements, well temperature measurements and  
445 previous surface mapping (Figure 25).

446 In January 2013, a shallow, corrosion-induced leak in the casing of PS-31 appeared. Consequently,  
447 steam production from PS-31 was halted. The well then received water injection initially at a high rate  
448 to condense the steam, and then at 300 gpm to keep the wellhead pressure at a negative value. The  
449 transition from 400 gpm water injection at P-32 to 300 gpm water injection at PS-31 occurred on  
450 February 13, 2013 and resulted in an immediate shift in the seismicity hypocenters that was entirely  
451 consistent with the location of the new PS-31 injection center (Figure 26). Injection into PS-31  
452 continued until March 21, 2013 when the well was suspended, the casing repaired and the wellbore  
453 capped by the injection of nitrogen.

454The Gutenberg-Richter Law is an empirical relationship between the magnitude  $x$  of a seismic event  
455and the total number of seismic events with magnitudes higher than  $x$  ( $N(x)$ ), and is generally  
456expressed as  $\log N(x) = a - b \cdot x$  (Gutenberg and Richter, 1942). The constant  $b$  is typically close to 1  
457for natural seismicity, and is typically higher for earthquake swarms (lacking a clear main shock), for  
458increasing material heterogeneity, for aftershocks, and for areas of having a high geothermal  
459temperature gradient (Kulhanek, 2005; Zang et al., 2014). This relationship is generally displayed in a  
460plot of seismic event magnitude vs.  $\log(\text{frequency } M \geq x)$ . A linear least-squares fit of 1,173 recorded  
461NW Geysers EGS Demonstration Project seismic events with magnitudes  $\geq 1.0$  has a “b-value” of  
4621.69 (Figure 27).

463

#### 4645.2 Non-condensable Gas Monitoring

465

466It is known that boiled injectate, or Injection derived steam (IDS) tends to dilute NCG concentrations  
467in The Geysers reservoir and to displace the original reservoir steam Beall et al. (2007). The result is  
468lower NCG and hydrogen sulfide ( $H_2S$ ) concentrations of produced steam. Stimulation monitoring  
469data show that the NCG concentrations of PS-31 steam, as well as the flow rate and shut-in well head  
470pressures (SIWHP) are controlled by SRGRP water injected in P-32.

471To monitor the effects of P-32 injection on the NCG concentrations of steam from the EGS  
472Demonstration area, samples from PS-31 and P-25 were periodically collected after water injection  
473began on November 6, 2001. The high NCG concentrations in PS-31 and P-25 made field sampling  
474problematic and resulted in some suspect samples. Due to the uncertainty in the data, NCG values  
475presented in this report have been averaged.

476Figure 28 shows the injection history of P-32 and the NCG concentrations of PS-31 and P-25 before  
477and after injection began. The first post-injection sample collected from PS-31 was during a flow test  
478on January 1, 2012, 117 days after injection had started and during the 1,000 gpm injection period.  
479The NCG concentration in PS-31 steam was 0.3 wt%, a reduction of about 92% from the pre-injection

480concentration of 4.5 wt%. This was the lowest NCG concentration measured at PS-31 during the  
481stimulation. At the end of the 700 gpm injection interval, the PS-31 NCG concentration during a flow  
482test showed a slight increase to 0.45 wt%. After injection into P-32 ceased (August 20, 2012 to  
483January 29,2013), the NCG concentration in PS-31 steam increased and peaked at 1.3 wt%. The  
484increase of NCG concentration is thought to be due to effects of PS-31 beginning production on  
485December 5, 2012 and no injection in P-32. During this period, the well was likely producing lower  
486amounts of low-NCG IDS and drawing in more high-NCG, native reservoir steam. Once P-32  
487injection restarted, the PS-31 NCG concentration dropped to 0.98 wt% in 14 days. Unfortunately, no  
488additional steam chemistry was obtained from PS-31 because production ceased in January 2013 after  
489a shallow casing leak appeared. The well is currently suspended, pending repairs. Nonetheless, the  
490data obtained clearly indicate a strong correlation between NCG concentration and the injection rate  
491into P-32. It appears that larger amounts of low-NCG IDS are generated in the reservoir and produced  
492at PS-31 as the P-32 injection rate increases. When the P-32 injection rate was reduced to less than  
493about 700 gpm, PS-31 NCG concentrations began to increase. A 1,000 gpm P-32 injection rate  
494resulted in the most significant PS-31 NCG concentration reductions. It has not been possible to test if  
495high-rate injection into P-32 can be sustained long-term without injection break-through occurring.  
496Figure 28 also shows the NCG concentrations of P-25, located northeast of the P-32 injector (Figure  
4972). More frequent geochemical monitoring was done for P-25 than PS-31 as it has been connected to a  
498power plant since December 9, 2011. The change in P-25 NCG concentrations in relation to P-32  
499injection has a very similar response to that measured at PS-31. The NCG concentrations for both  
500wells decreased dramatically after P-32 injection started, leveled out as the injection rate dropped from  
5011,000 gpm to 700 gpm, and then increased significantly after P-32 injection ceased. The magnitude of  
502the initial NCG concentration decrease after production started was slightly larger for PS-31 than P-25  
503(92% versus 88%). However, P-25 had a much longer delay in resuming a decreasing trend after the  
504restart of P-32 injection on January 29, 2013. NCG concentrations of PS-31 responded to the injection  
505restart within 14 days, whereas, P-25, responded between days 72 through 139. A comparison of the P-

50625 and PS-31 NCG response suggests a more robust reservoir connection between P-32 and PS-31  
507than with P-25.

508NCG concentrations in produced steam are obtained for all production wells in The Geysers annually.  
509The distribution of NCG concentrations in the greater EGS Demonstration area is shown in the  
510contour map in Figure 29 prior to injection in P-32 and 2 months after the start of stimulation. Note  
511the elongate northeast-southwest NCG low (10,000 ppmw contour) that developed around injector P-9  
512in 2010. This well has been injecting since late 2007 and developed a large cell of IDS in the reservoir  
513that did not appear to extend into the EGS Demonstration area. Once P-32 injection started, this NCG  
514low enlarged significantly westward and northward. There are currently no existing production wells  
515located to the northwest of the EGS Demonstration area, so it is difficult to accurately determine the  
516area impacted by injection.

517

### 5185.3 Chloride Monitoring

519

520A chloride concentration of steam above about 1 ppmw is known to have the potential to cause  
521corrosion in surface and near-surface piping, especially when the superheat of steam is  $\leq 40^{\circ}\text{F}$ . Based  
522on the knowledge of existing north Geysers production wells having chloride concentrations above 1  
523ppmw, chloride analysis was included as part of the EGS Demonstration geochemical monitoring. It  
524must be noted that steam chloride concentrations can vary widely due to condensate films that can bias  
525results, and trends can be difficult to ascertain. All steam condensate samples were collected with a  
526probe inserted into the center of the wellbore or test pipeline.

527During flow testing and production of PS-31, the steam chloride concentrations ranged between a low  
528of 0.67 to a high of 135 ppmw (Table 1). It is apparent that as injection into P-32 progressed, an  
529obvious decrease in chloride concentration did not occur in parallel with the decrease achieved in  
530NCG concentration. Within 10 weeks after PS-31 went into production on December 5, 2013, the  
531casing corroded and developed a hole about 4.6 m (15 ft) below the surface. We suspect that P-32

532 injection has not saturated the rock matrix near PS-31, as saturation could possibly scrub or reduce  
533 chloride concentrations. As a consequence, dry superheated steam paths may still extend from the  
534 HTR into the overlying PS-31 NTR. A caliper log run on June 25, 2012 and prior to PS-31 production  
535 showed the casing to be in good condition. A caliper log made after the near-surface leak was  
536 discovered, and only 10 weeks after the production of PS-31 began, shows significant corrosion to a  
537 depth of 2,500 ft, with a maximum corrosion rate of 100 mil/year (1 mil=0.001 inch) at 305 m (1000  
538 ft) depth. The repair of PS-31 is planned for mid-2016 and includes the installation of a corrosion-  
539 resistant high alloy steel (2507) liner to a depth of approximately 1220 m (4000 ft).

540

#### 541 5.4 Stable Isotope Monitoring

542

543 The relationship between meteoric water flushing and whole-rock oxygen isotope values was  
544 integrated into the understanding of the relationship between the HTR and NCG concentration  
545 throughout the north-west Geysers ([Walters and Beall, 2002](#)). They described an area of the  
546 Northwest Geysers (specifically the EGS Demonstration area) where extremely high NCG  
547 concentrations (up to 7 wt%) and isotopically heavy ( $\delta^{18}\text{O}$ ) reservoir metagraywacke indicate  
548 a lack of flushing by meteoric water.

549  $^{18}\text{O}$  and deuterium (D) are natural tracers which allow the determination of the  
550 percentage of injection-derived water versus native water. Because there is a very large  
551 isotopic difference in the  $\delta^{18}\text{O} / \delta\text{D}$  ratio between meteoric water and the native EGS fluid  
552 which is at least partially connate water, isotopic analysis has been used to trace the P-32  
553 injection water rather than conventional tracer methods.

554 The native steam from P-25 and PS-31 had  $\delta^{18}\text{O}$  values of about +2 per mil and  $\delta\text{D}$  values of  
555 about -48 per mil when these wells were originally flow tested in the 1980s. These  $\delta^{18}\text{O}$  values  
556 are indicative that the native steam in these areas was not significantly influenced by meteoric

557water. Various geochemical and fluid inclusion studies (Haizlip, 1985; Moore and Gunderson,  
5581995; Truesdell et al., (1994); Moore et al., 2001; Walters and Beall, 2002; and Lowenstern and  
559Janik, 2003) have concluded that the early steam in these areas was from connate water (sea  
560water trapped in the metagraywacke and argillite reservoir rocks) from the Mesozoic Era  
561(about 150 million years ago). The  $\delta^{18}\text{O}$  values in Standard Mean Ocean Water (SMOW) have  
562not varied significantly from 0 per mil for the last 150 million years, the approximate age of  
563the Franciscan Assemblage rocks at The Geysers.

564The  $\delta^{18}\text{O}$  values in steam produced from P-25 and PS-31 in 2012 have decreased from about  
565+2 per mil to about -2 per mil and -4.5 per mil, respectively, in 2012. The Santa Rosa Geysers  
566Recharge Project (SRGRP) water injected since 10/6/11 has  $\delta^{18}\text{O}$  values of -6 per mil and  $\delta\text{D}$   
567values of -38 per mil, very similar to the local meteoric waters in the northwest Geysers. The  
568 $\delta^{18}\text{O}$  and  $\delta\text{D}$  values of local meteoric water, SRGRP water, the original steam produced from  
569the northwest Geysers, and the steam from the EGS Demonstration production wells, PS-31  
570and P-25 are plotted in Figure 30.

571The mixing-line in Figure 30 indicates that by January 2013, only three months after the  
572injection of SRGRP water into P-32 began, about 80 percent of the steam from PS-31 was  
573injection-derived steam (IDS) from SRGRP water and about 45 percent of the steam from P-  
57425 was IDS. Therefore, it is evident that the IDS from SRGRP water injected into P-32  
575resulted in flushing of the EGS Demonstration reservoir.

576Injection into P-32 ceased from August 20, 2012 until January 29, 2013. As a result the  $\delta^{18}\text{O}$   
577values in PS-31 and P-25 steam increased about 2 per mil, and the mixing-line indicates that  
578about 45% of the steam from PS-31 is IDS, and 25% of the steam from P-25 is IDS.



579Therefore, like the NCG concentrations, the stable isotope concentrations in the EGS steam  
580are a function of the SRGRP injection rates in P-32.

581Three maps for the EGS project area and vicinity are presented in Figures 7 and 31: (1) early  
582(1977-1985)  $\delta^{18}\text{O}$  values; (2)  $\delta^{18}\text{O}$  values in the Caldwell Ranch project area acquired in 2010  
583and early 2011 from recently re-opened and recompleted wells; and (3)  $\delta^{18}\text{O}$  values acquired  
584in 2012 after P-32 began injecting SRGRP water. These maps show that the  $\delta^{18}\text{O}$  values of  
585steam in the western half of the Caldwell Ranch project area and the southeastern part of the  
586EGS Demonstration area has been progressively, and substantially, reduced by the injection of  
587SRGRP water at P-32 and P-9: from 0 to +3 per mil before 2010 to -1 to -4 per mil in 2012.

588After the injection of SRGRP water into P-9 began in November 2007, the  $\delta^{18}\text{O}$  values of the  
589steam produced from the western half of the Caldwell Ranch project decreased from the range  
590of 0 to +2 per mil to the range of -1 per mil. It is noted that P-9 water injection did not change  
591the  $\delta^{18}\text{O}$  values in the EGS Demonstration area where the heavy  $\delta^{18}\text{O}$  values ranging from +1  
592to +3 in the native steam remained unchanged (Figure 31).

593

## 5946 **LESSONS LEARNED FROM STIMULATION**

595

596Lessons learned and the successful practices developed in stimulating the reservoir around P-32 are  
597included in this section. The goal of stimulation is to enhance the natural permeability through the  
598injection of fluids (Tester et al., 2006). The creation of an EGS reservoir may be achieved by two  
599methods: (1) high pressure hydraulic fracturing to create new fractures over a very short period of time  
600(hours), or (2) the shear reactivation of pre-existing fractures at relatively low pressures just high  
601enough to cause shear failure over a long time period (months). At the northwest Geysers modeling  
602indicates that shear reactivation of pre-existing fractures is triggered by the combined effects of

603 injection-induced cooling around the injection well and rapid (but small) changes in steam pressure as  
604 far as half a kilometer from the injection well ([Rutqvist et al. \(2015a\)](#), [this issue](#)).

605

#### 606 **6.1 Community impact and outreach**

607  
608 Project awareness and community support for this project was achieved through public meetings, a  
609 dedicated EGS website, access to the Calpine Geothermal Visitor Center (upgraded in 2012) and EGS  
610 update presentations at regular intervals.

611 The Northwest Geysers EGS Demonstration project is located 10.5 and 14.5 kilometers (6.5 and 9  
612 miles), respectively from the Cobb and the Anderson Springs communities. Techniques for the  
613 stimulation of geothermal reservoirs are being refined, and it is advantageous for EGS test programs to  
614 be sited at a distance from communities. There have been a total of eight seismic events associated  
615 with the EGS Demonstration with  $M \geq 2.50$ , the largest of these being an  $M 3.74$  on January 21, 2014  
616 and an  $M 2.87$  on May 31, 2012. The timing of these  $M \geq 2.50$  seismic events does not show a  
617 particularly strong correlation with injection rate or injection rate variability. The  $M 3.74$  event  
618 resulted in a geometric mean peak ground acceleration (PGA) value of  $11.87 \text{ cm/sec}^2$  (1.2% of  
619 gravitational acceleration ( $g$ )) at the Anderson Springs Strong Motion Station. According to USGS  
620 guidelines, this is consistent with a Modified Mercalli Intensity of IV (light perceived shaking and no  
621 potential for damage). The Cobb Strong Motion Station was offline due to a memory card failure, and  
622 estimated to have a geometric mean peak ground acceleration in the range of  $18.0$  to  $24.0 \text{ cm/sec}^2$  (1.8  
623 to 2.4% of  $g$ ), consistent with a Modified Mercalli Intensity of IV (light perceived shaking and no  
624 potential for damage). The  $M 2.87$  seismic event, the second largest in the EGS Demonstration area  
625 since injection began, resulted in negligible geometric mean PGA values of  $1.53 \text{ cm/sec}^2$  (0.16% of  $g$ )  
626 at Anderson Springs and  $1.38 \text{ cm/sec}^2$  (0.14% of  $g$ ) at Cobb; these PGA values are consistent with a  
627 Modified Mercalli Intensity of I (no perceived shaking and no potential for damage).

628

## 6296.2 Well Testing and Well Logging

630

631The addition of observation wells to the EGS injection-production well pair, P-32 and PS-31,  
632respectively have proved to be very important to monitoring the EGS demonstration. Static pressure  
633monitoring wells (i.e., WHS-71, P-25, and P-38) outside of the immediate EGS reservoir area  
634provided constraints on the size of the stimulated, EGS reservoir volume. Pressure transient analysis  
635proved to be a valuable tool in assessing the increased permeability near PS-31.

636A tight seal of the wireline lubricator at the P-32 well head was not achieved during the initial PT  
637logging and resulted in steam leakage during this survey. As a consequence, the results were noisy and  
638created difficulties during analysis.

639High temperature well logging tools are needed to accurately characterize the reservoir before  
640stimulations and to track the stimulation process. The standard injectivity test at The Geysers differs  
641from testing used in other reservoir types. A 'falling head' injectivity test could have provided us with  
642an estimated flow rate of injected fluid getting into the reservoir to better assess the permeability of the  
643well. This type of survey could have benefited from a surface read-out tool. Due to high temperature  
644in the wells we were limited to the use of memory tools for logging. The limitation of 180°C (350°F)  
645for casing caliper tools prevented the use of these to depths more than 600 m (2000 ft)

646

## 6477 CONCLUDING REMARKS

648Phase I of the EGS Demonstration Project has been completed. Two previously abandoned wells, PS-  
64931 and P-32 were reopened and deepened as an EGS production-injection well pair in the HTR. PS-31  
650was completed as a production well that can communicate with both the NTR and the HTR. P-32 was  
651completed as an injection well designed to inject water at low pressure and low flow rates in the HTR.  
652A pipeline was built to carry tertiary-treated waste water from the Santa Rosa Geysers Recharge  
653Pipeline to P-32.

654 Injection in P-32 has resulted in a substantial reservoir pressure rise in the area compared to values  
655 observed in the 1980s. The stimulation has also caused an increase in the flow rate at P-25 and a  
656 considerable reduction of the NCG concentration in the P-25 steam. The maximum NCG drop in PS31  
657 and P25 occurred at injection rates of 1000 gpm in P32. Pressure transient analysis of PS-31 flow rate  
658 indicates that the kh increased to 42,300 md-ft (12.69 Dm) following stimulation from the 22,000 md-  
659 ft (6.6 Dm) value found when the well was re-opened. This increase is considered small but it is an  
660 indication that permeability has increased at the EGS site, albeit at a low rate.

661 Comprehensive seismic data collection and analysis has been an integral part of the EGS  
662 Demonstration Project, primarily utilizing the LBNL field-wide permanent seismic monitoring  
663 network, along with two program-specific temporary LBNL seismic monitoring networks. A  
664 seismicity cluster began to develop almost immediately after P-32 water injection was initiated, and  
665 data analysis indicates; (1) the opening of new permeability zones defined by seismicity that are  
666 confined in time/space; (2) preferential water movement NNW (N130) trending along tilted zones of  
667 permeability; (3) limited water flow to the southeast and northeast which correlates with surface  
668 faulting; (4) the downward progression of seismicity indicating deeper permeability stimulation,  
669 particularly at the 1,000 gpm injection rate; and (5) increased seismicity associated with an injection  
670 rate increase, followed by a significant decrease in event frequency.

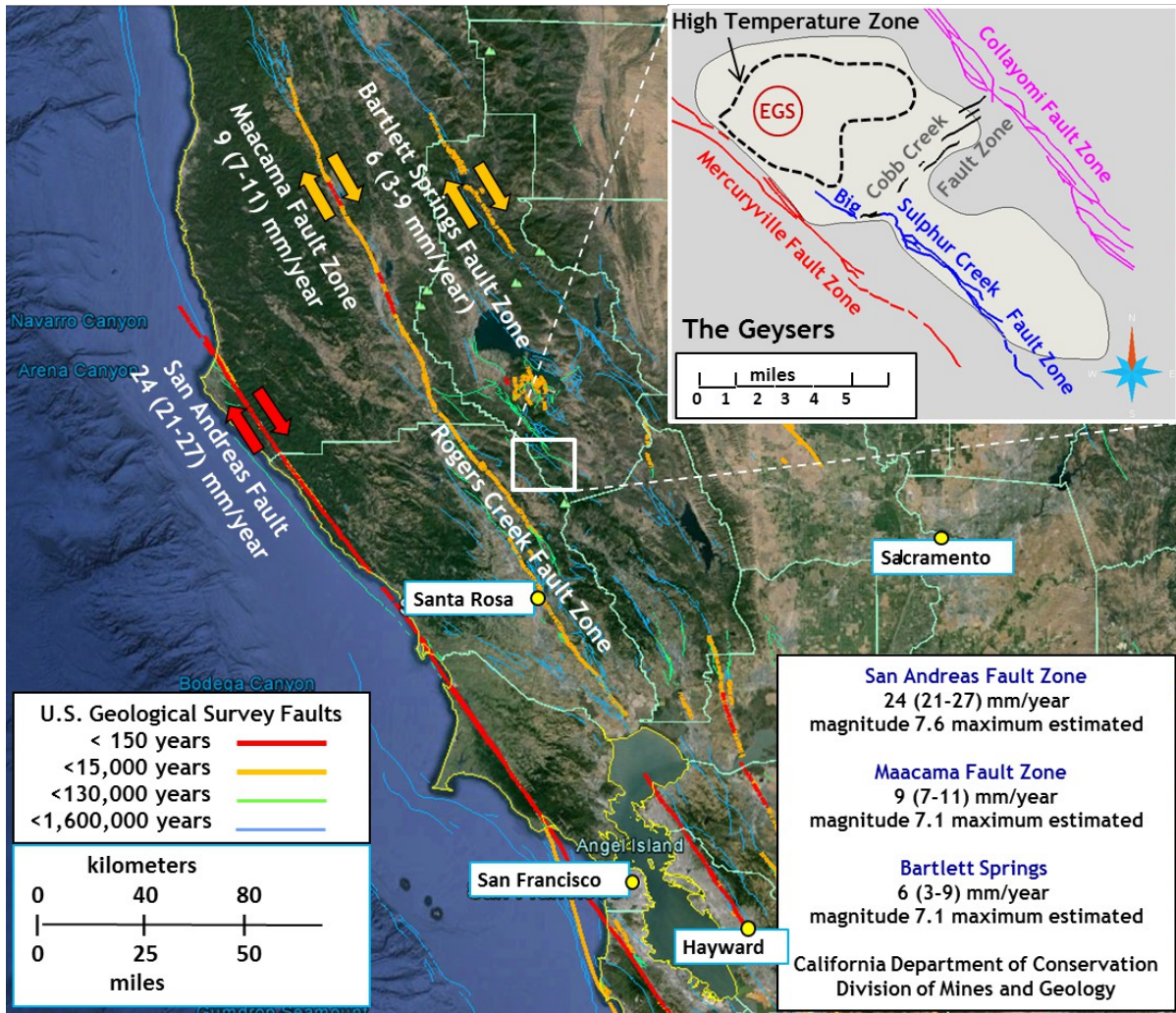
671 Injection is expected to continue through 2017. PS-31, P-32, and other area wells will be continuously  
672 monitored, periodically flow tested or injection tested, and sampled for geochemistry. Seismic data  
673 will also be collected continuously and analyzed on an ongoing basis.

674

## 675 **ACKNOWLEDGMENTS**

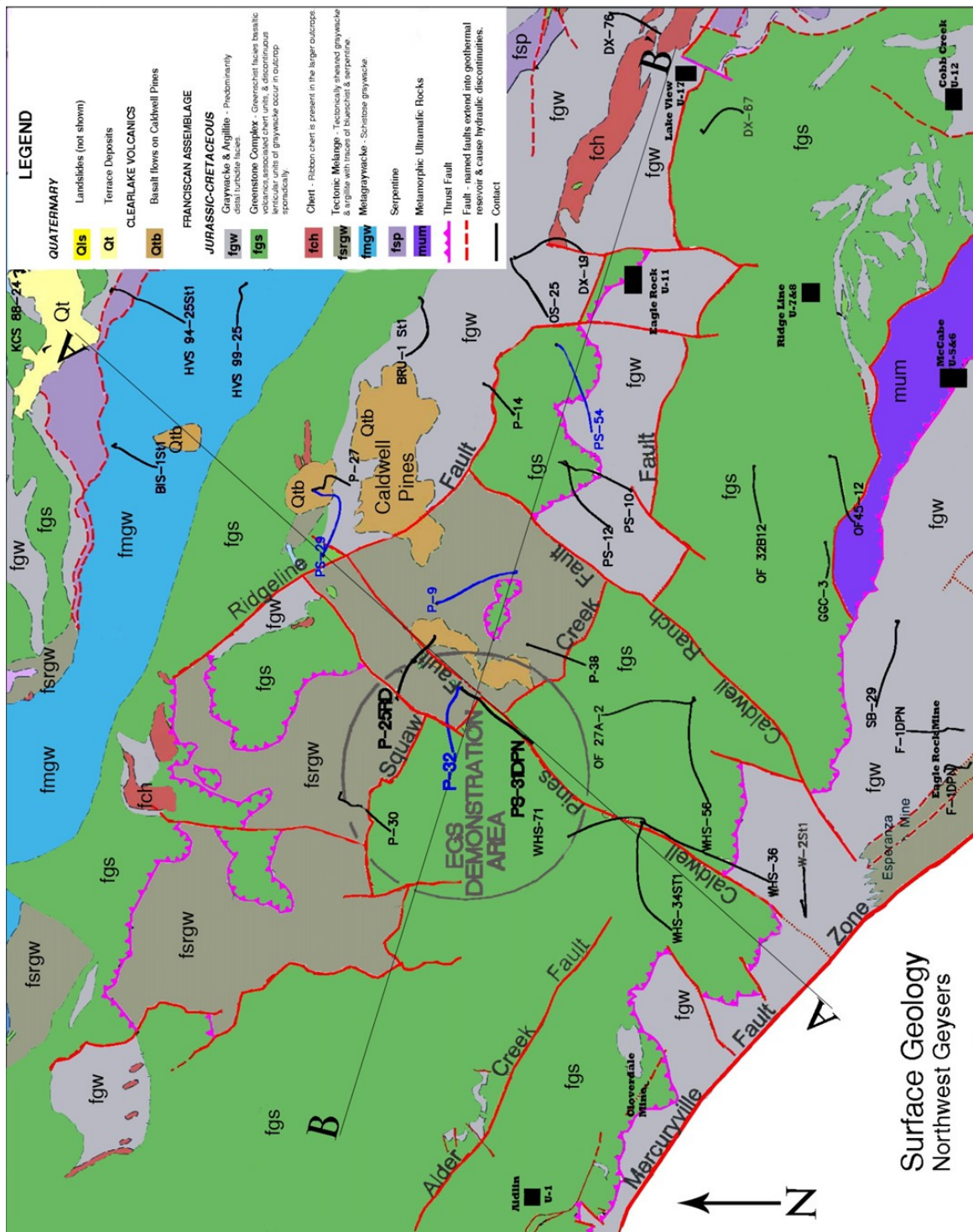
676 This work was conducted with funding by the Assistant Secretary for Energy Efficiency and  
677 Renewable Energy, Geothermal Technologies Program, of the U.S. Department of Energy under the  
678 U.S. Department of Energy Contract No. DE-FC36-08G018201, and by Calpine Corporation.

679  
 680  
 681  
 682



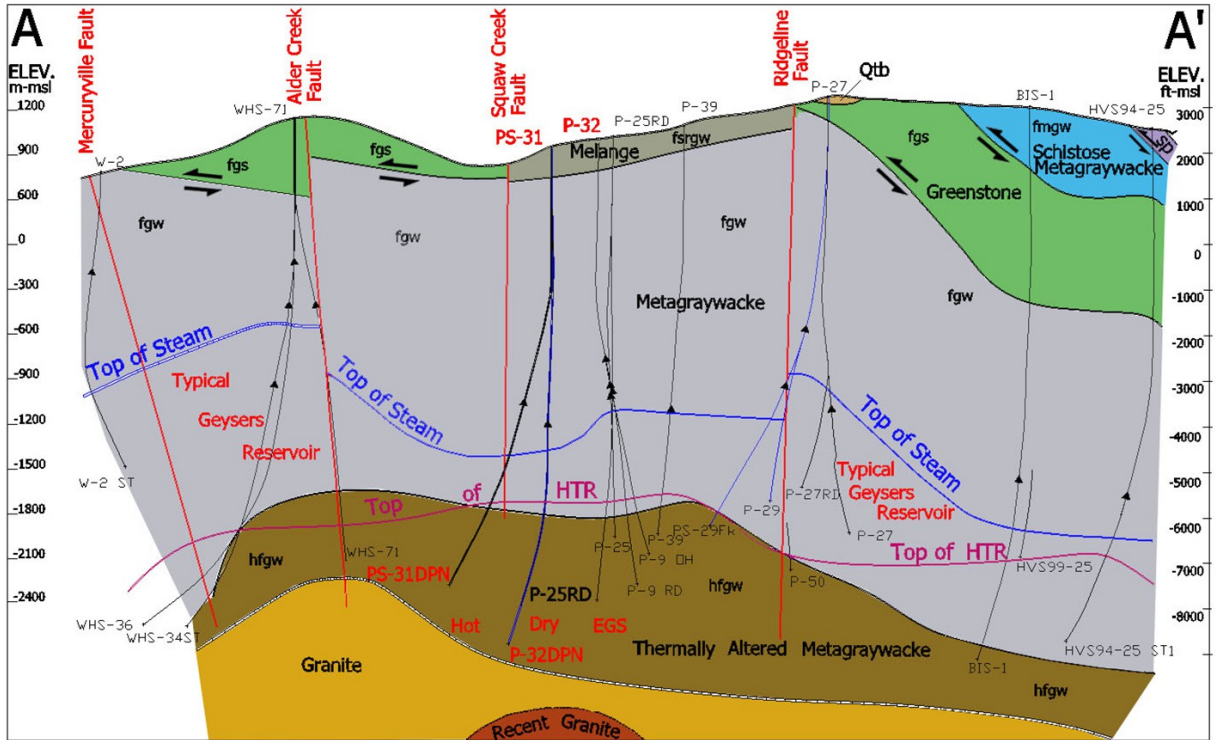
683Figure 1: The San Andreas Fault System, including the Maacama / Rodgers Creek Fault Zone and  
 684Bartlett Spring Fault Zone. Only faults with activity in the previous 15,000 years are displayed  
 685(California Division of Mines and Geology, 1996). The inset map shows the location of the EGS  
 686Demonstration Project and the surrounding high temperature region of the northwest Geysers.





688Figure 2: Surface geology of the Northwest Geysers EGS Demonstration Area. Surface faults in the  
 689Northwest Geysers which are coincident with hydraulic discontinuities in the reservoir are labeled in  
 690red. The hydraulic discontinuity between the EGS Demonstration Area and Caldwell Ranch project is  
 691attributed to the Caldwell Pines Fault shown above. The locations of geologic cross-section (A-A') and  
 692rock isotope cross sections (A-A' and B-B') are shown in Figures 3, 5 and 6).  
 693

694



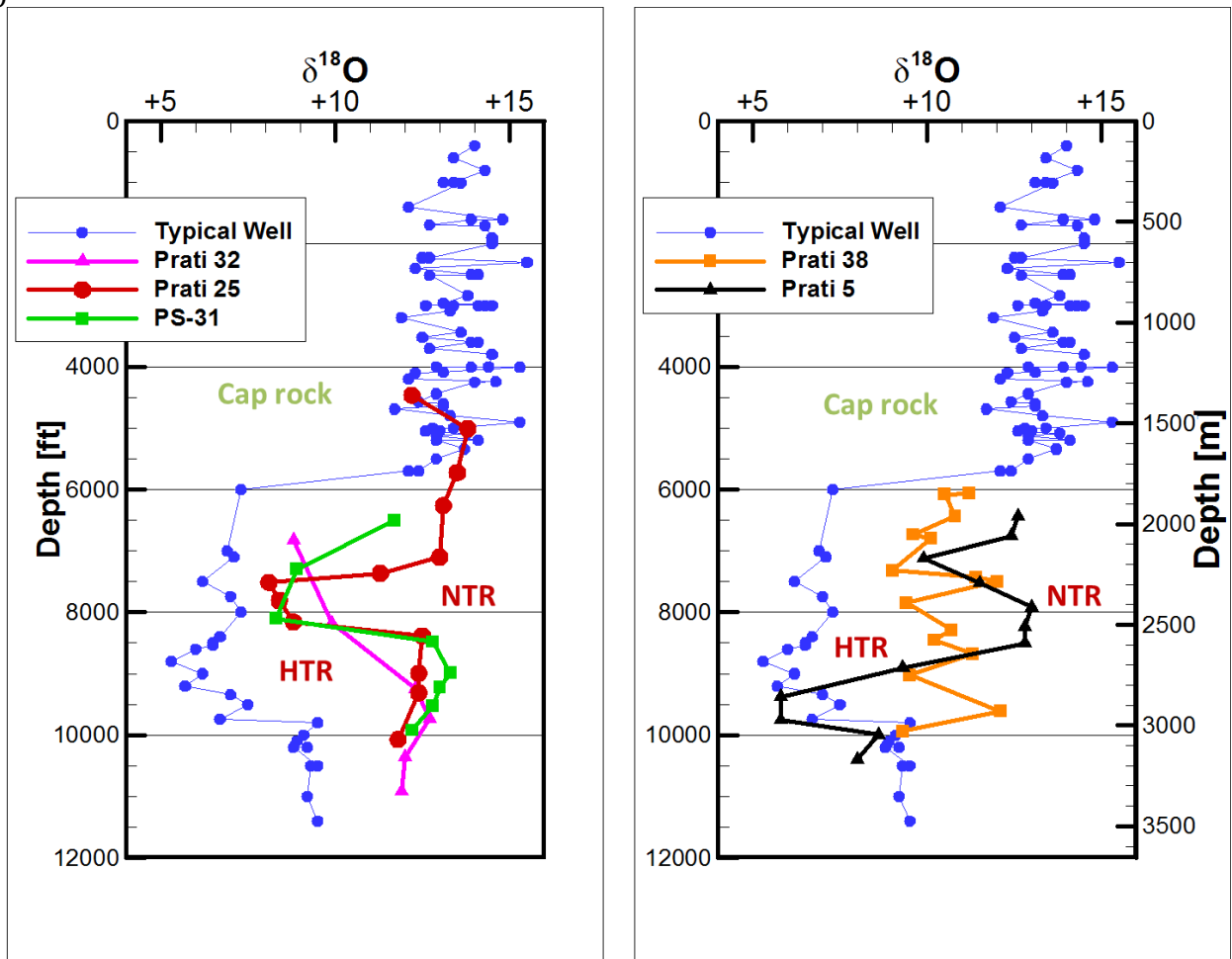
695

696 Figure 3: Geologic cross-section (A-A') of the Northwest Geysers and location of the EGS

697 Demonstration Area. Line of cross section is shown in Figure 2

698

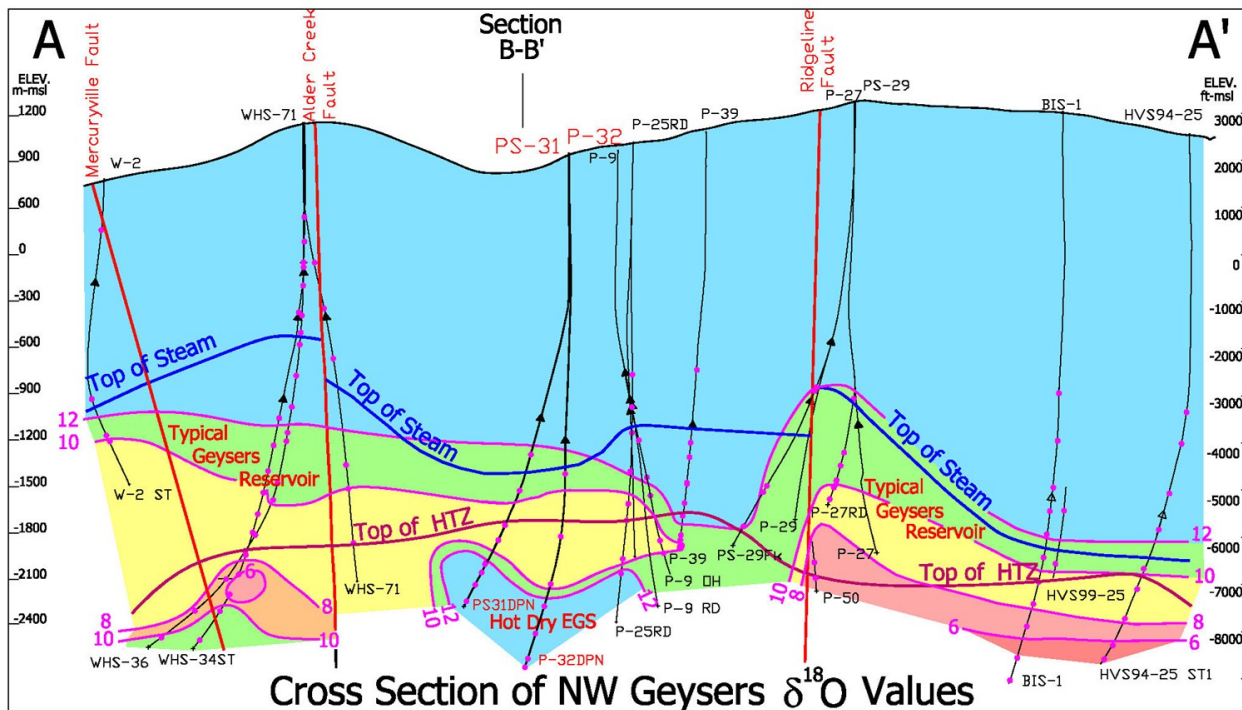
699



700

701 Figure 4: Whole-rock  $\delta^{18}\text{O}$  values for the Northwest Geysers are plotted versus depth. The graph is for  
702 the EGS Demonstration reservoir wells shown in color and a typical Northwest Geysers reservoir well.  
703 The Typical Well plot (shown in gray above) is a composite of NTR wells that surround the EGS  
704 Demonstration area. Note that the HTR rocks in the Caldwell Ranch, which are in a different reservoir  
705 compartment than the EGS wells, are exchanged with meteoric water. (After Lutz et al. (2012))

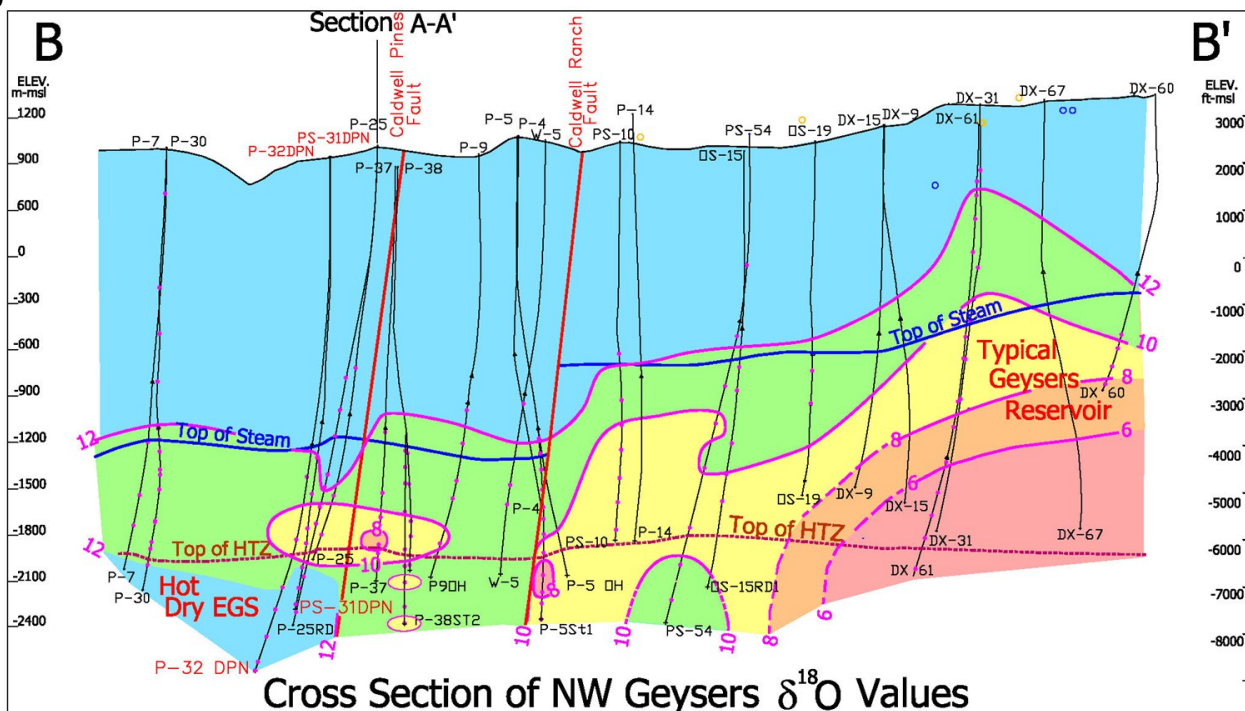




707

708 Figure 5: Southwest to Northeast Cross Section B-B' through the EGS Demonstration area.

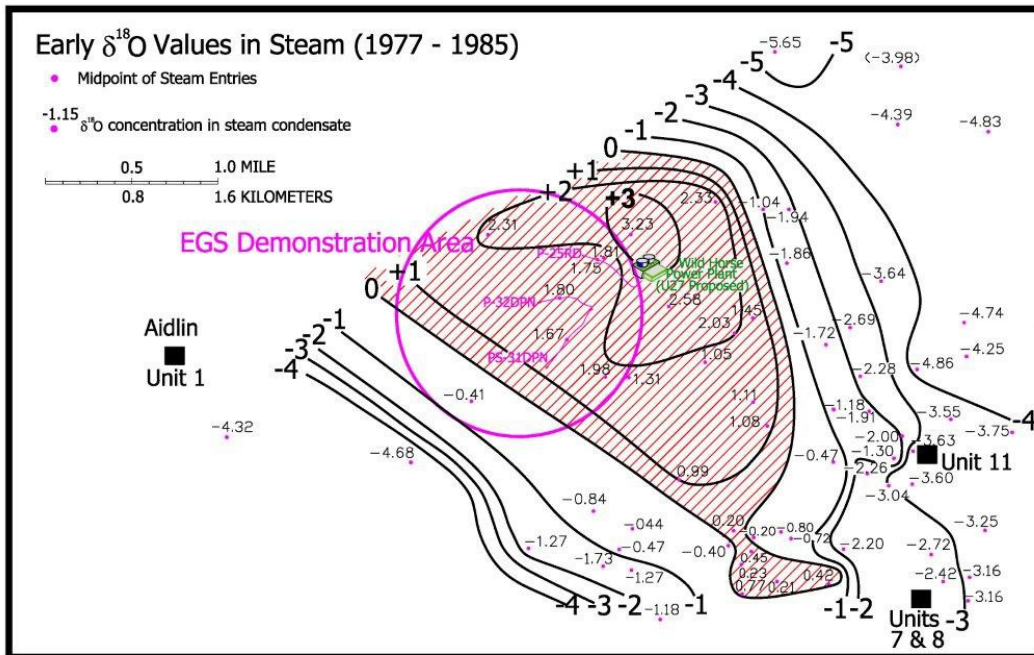
709



711

712 Figure 6: Northwest to Southeast Cross Section C-C' through the EGS Demonstration area.

713

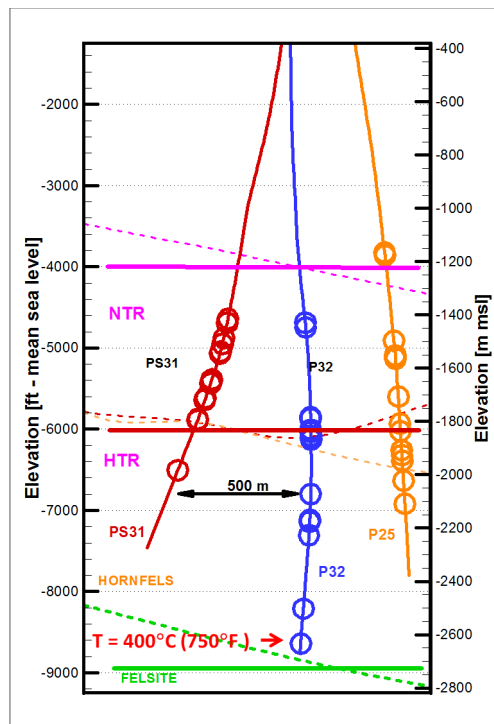


714

715 Figure 7: Early (1977-1985)  $\delta^{18}\text{O}$  Isotope Values in Northwest Geysers Steam Condensate.

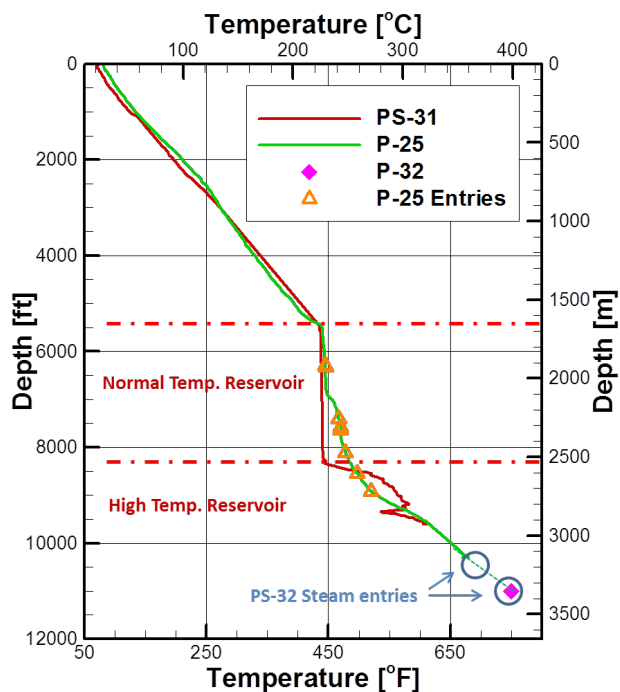
716

717



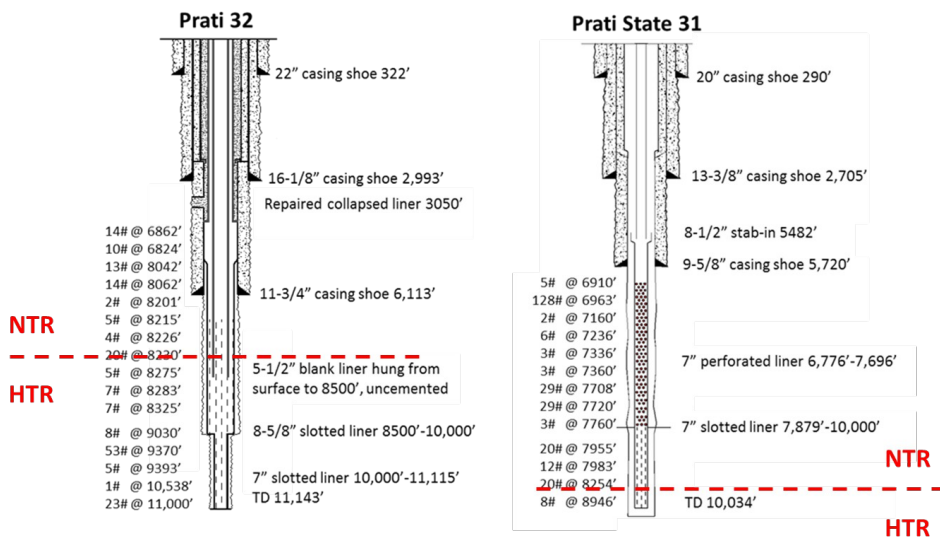
718 Figure 8: Cold water injected into P-32 (blue) is produced from PS-31 (red). Circles represent steam  
719 entries.

720



722 Figure 9: Static temperature profiles for P-25 (green line, temperature profile; orange triangles,  
 723 location of P-25 steam entries) and PS-31 based on pressure-temperature logs. Maximum recorded  
 724 temperature for P-32 indicated by magenta diamond and an extrapolated temperature profile in P-32  
 725 represented as a blue dashed line.

726  
 727



728 Figure 10: Left: P-32 completion schematic; Right: PS-31 completion schematic (not to scale). The  
 729 relative force of the steam entries (psig, #) upon the pressures of the compressed air used in drilling  
 730 wells and the measured depth at which these were encountered are listed to the left of the wellbore  
 731 schematic above

732



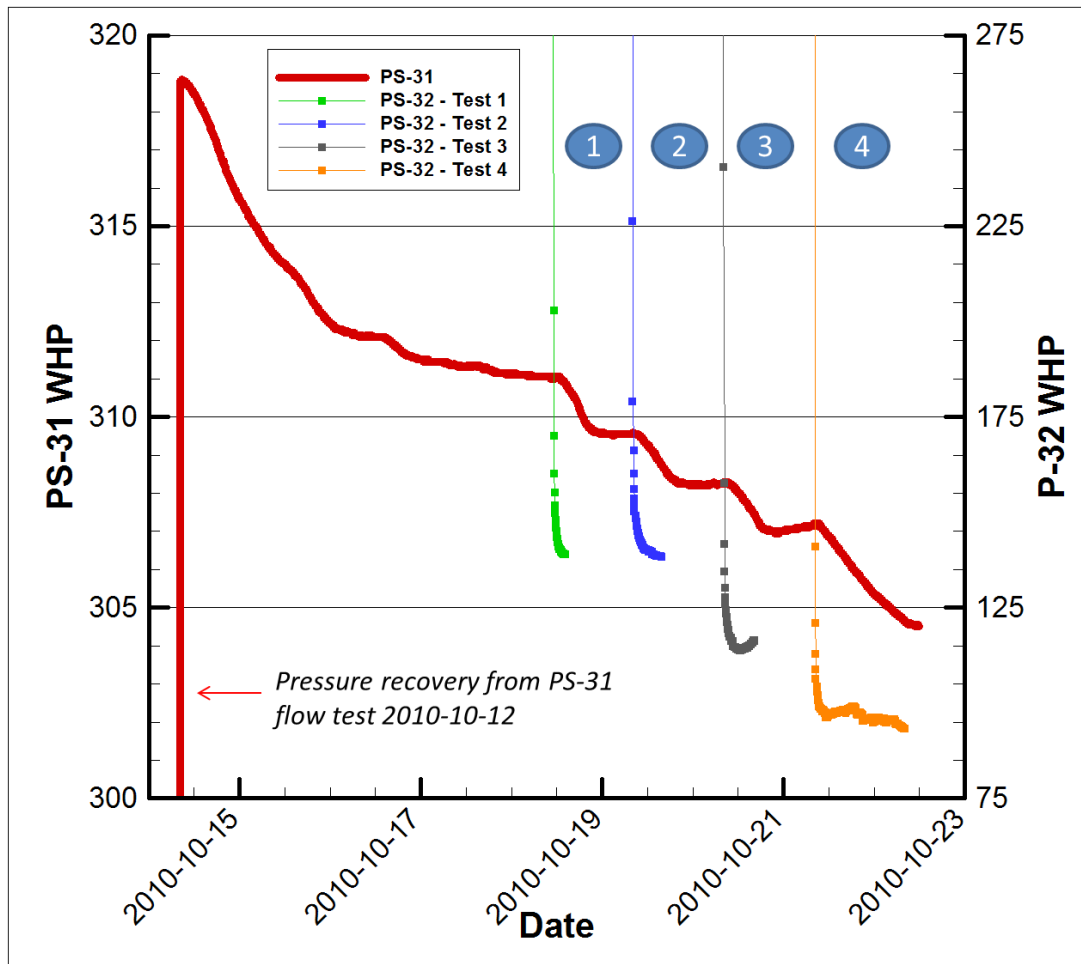
733

734

735 Figure 11: Average bit condition after 91.4 m (300 ft) of typical air drilling in the normal temperature  
736 Geysers reservoir (left) and Prati 32 final bit condition after 30.5 m (100 ft) of air drilling to a final  
737 depth of 3396 m (11143 ft) in the high temperature reservoir.

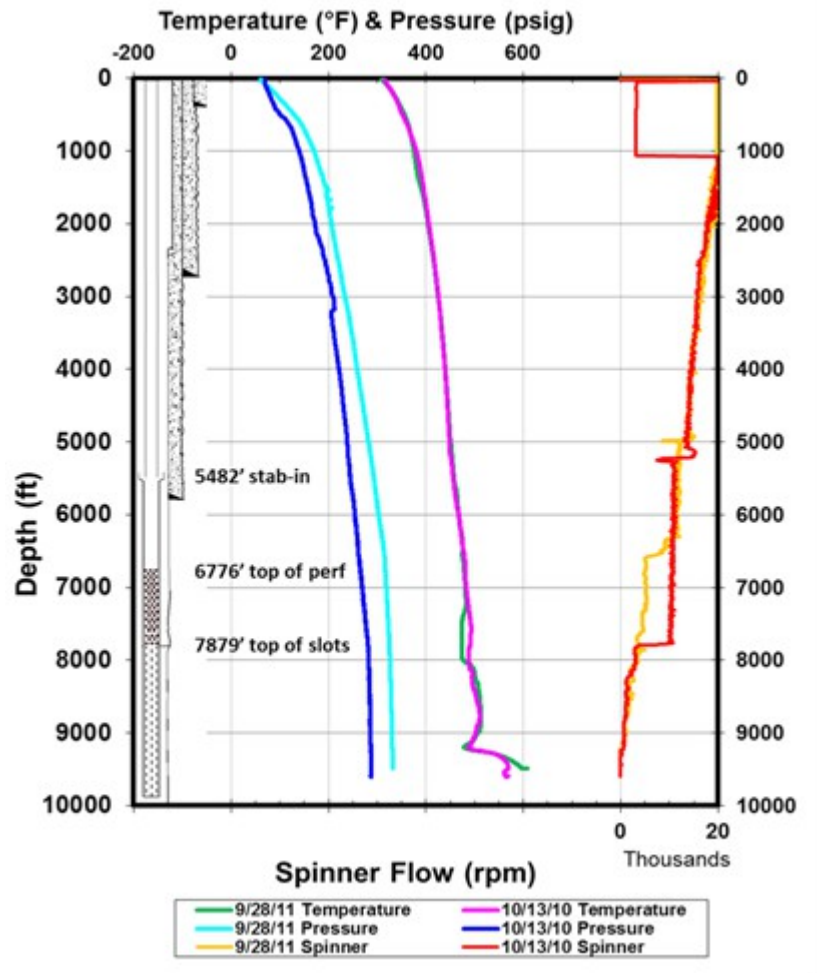
738

739



740 Figure 12: Wellhead pressure at PS-31 and pressure interference during isochronal flow tests at P-32  
741 (2010-10-18 and 2010-10-22): WHP {psig}/ Flow Rate {KPH} at P-32 (1) 137.7/83.2, (2) 115.8/86.4,  
742 (3) 96.9/87.6, and (4) 92.8/85.0.

743  
744



745  
746  
747

Figure 13: Flowing pressure-temperature-spinner (PTS) logs in PS-31(10/13/10 and 9/28/11)



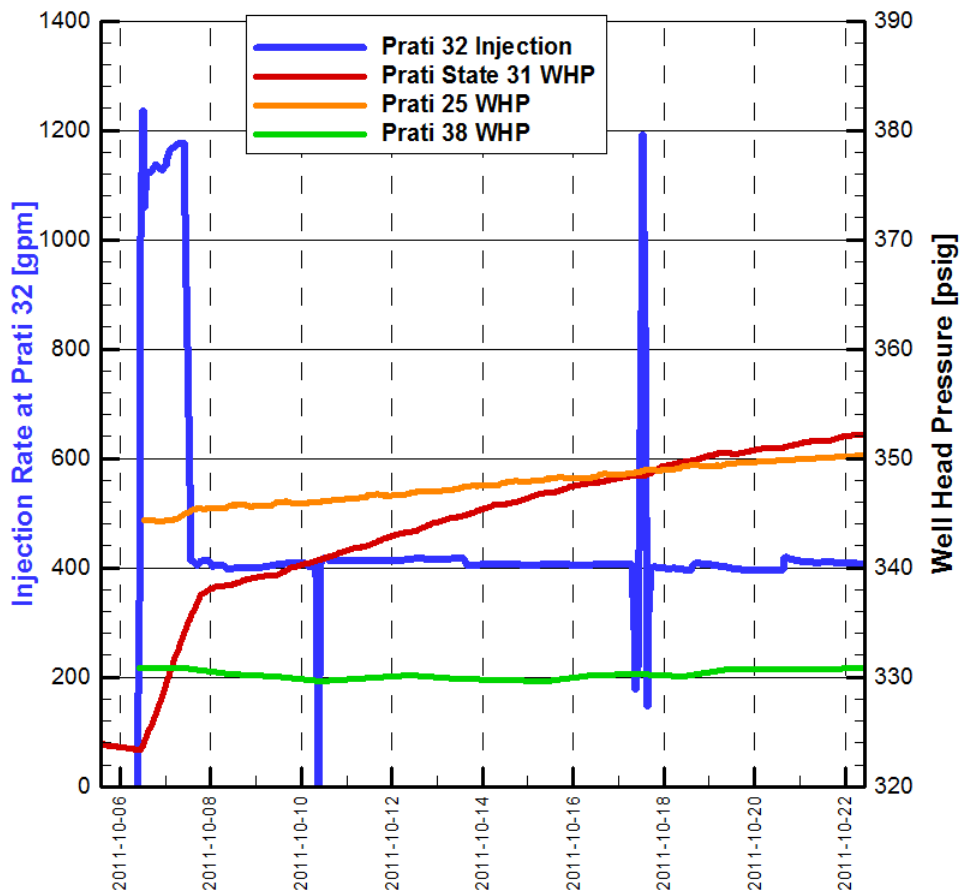
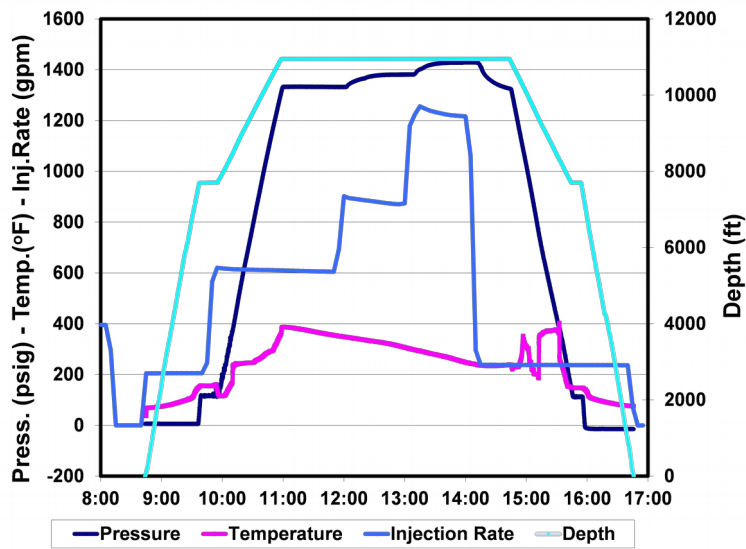


Figure 14: P-32 injection startup and well head pressures in P-25, PS-31 and P-38.

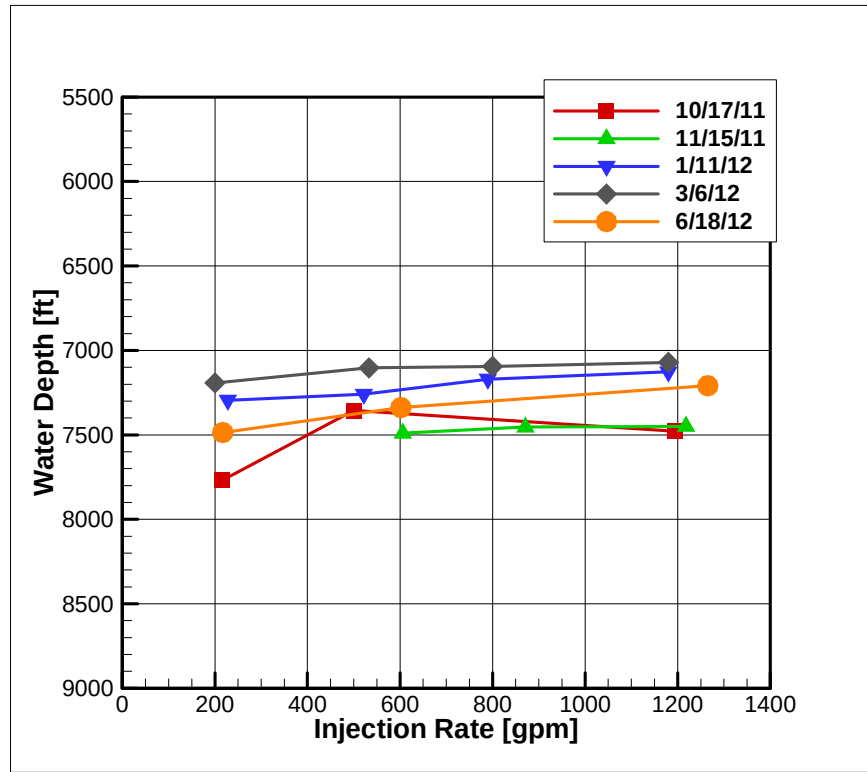
748  
749  
750  
751



752  
753  
754  
755  
756

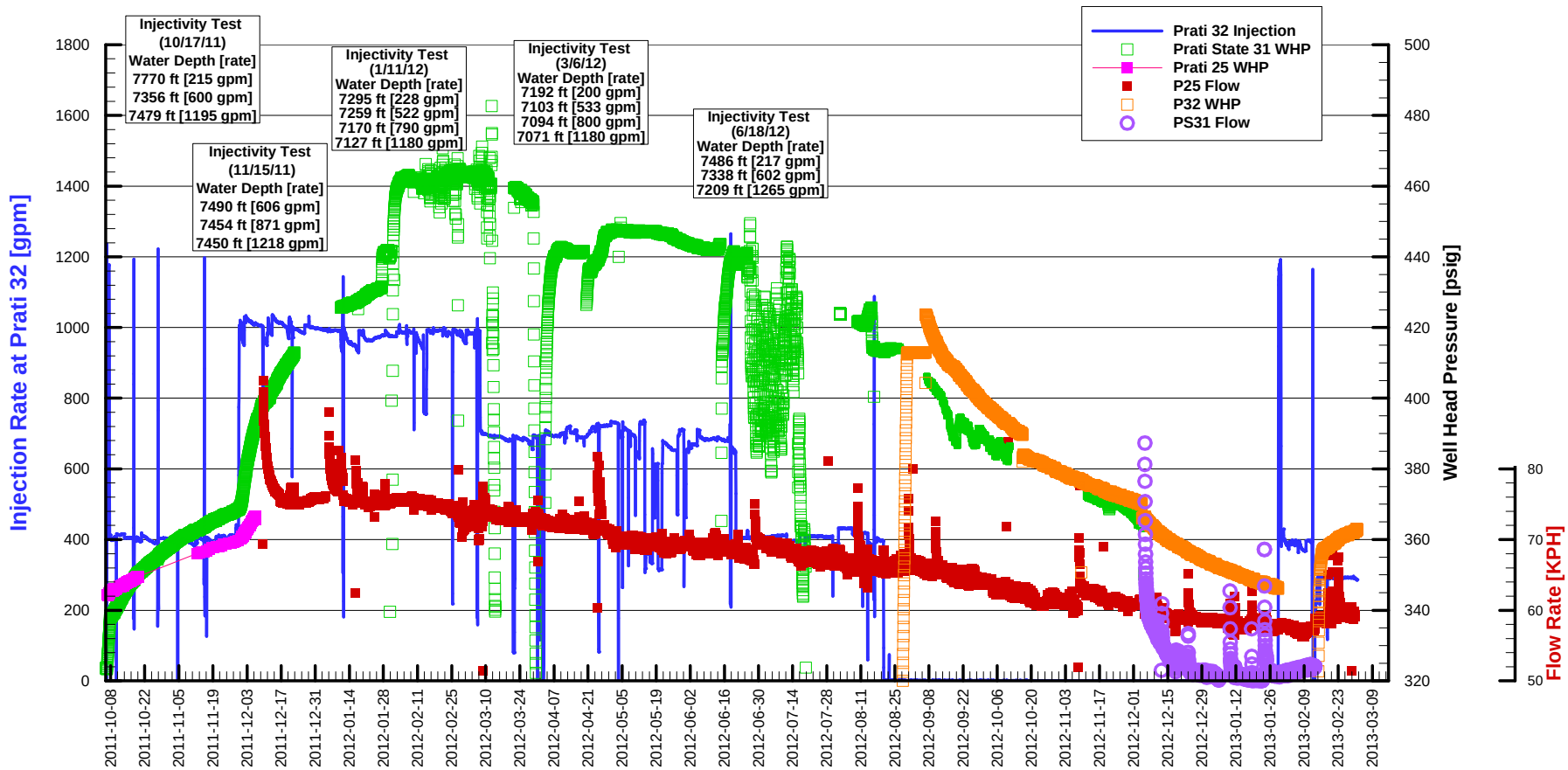
Figure 15: P-32 step-rate injectivity test on 11-15-11. PT tool hung at 10,950 ft during three injection rate steps (between 10:45 and 15:00). Light blue indicated PT tool depth as it traverses the well bore.

757



758  
759  
760  
761  
762

Figure 16: P-32 injectivity test. Lines represent depth of water table in the well measured from surface. Higher depth for a given rate indicates higher injectivity.

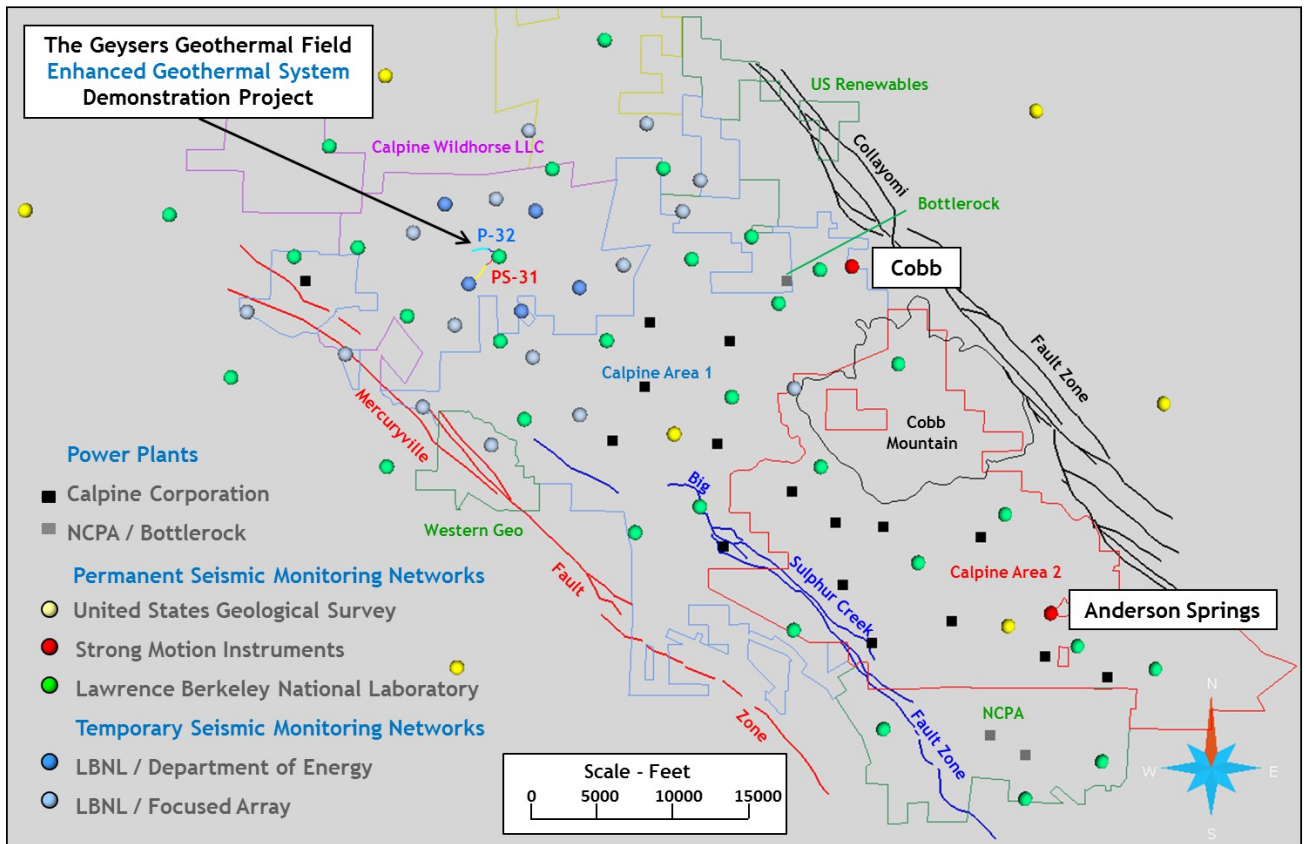


763  
764  
765

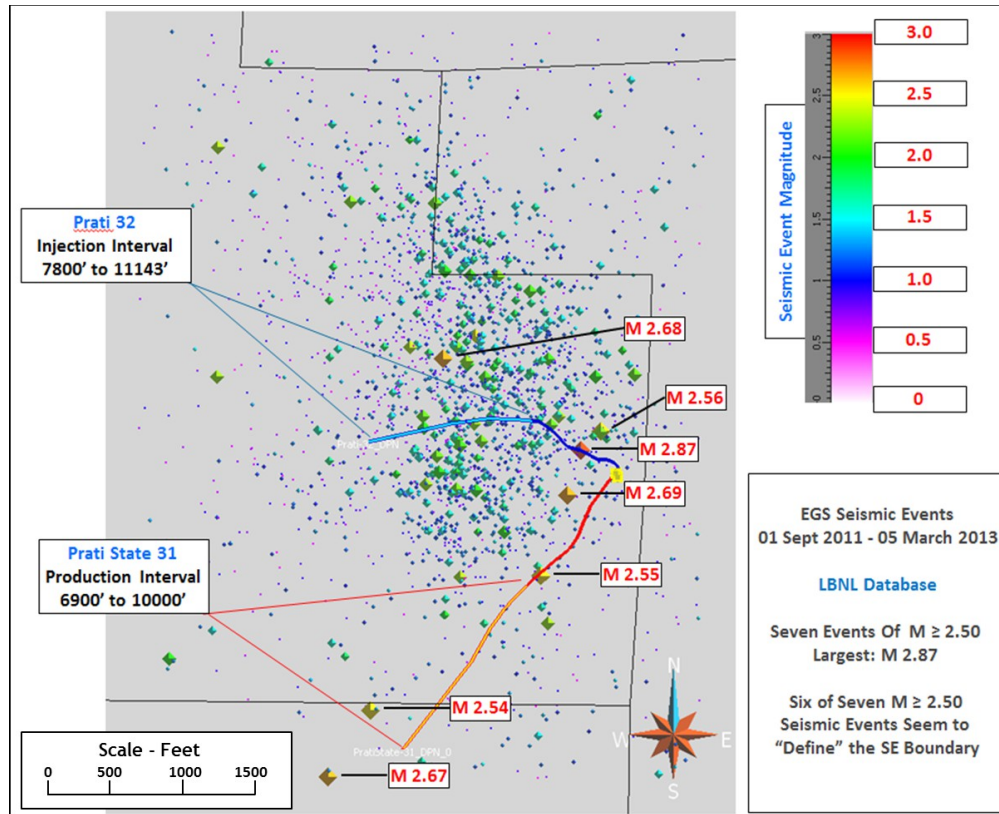
Figure 17: P-32 injection and well head pressure at PS31 and P25



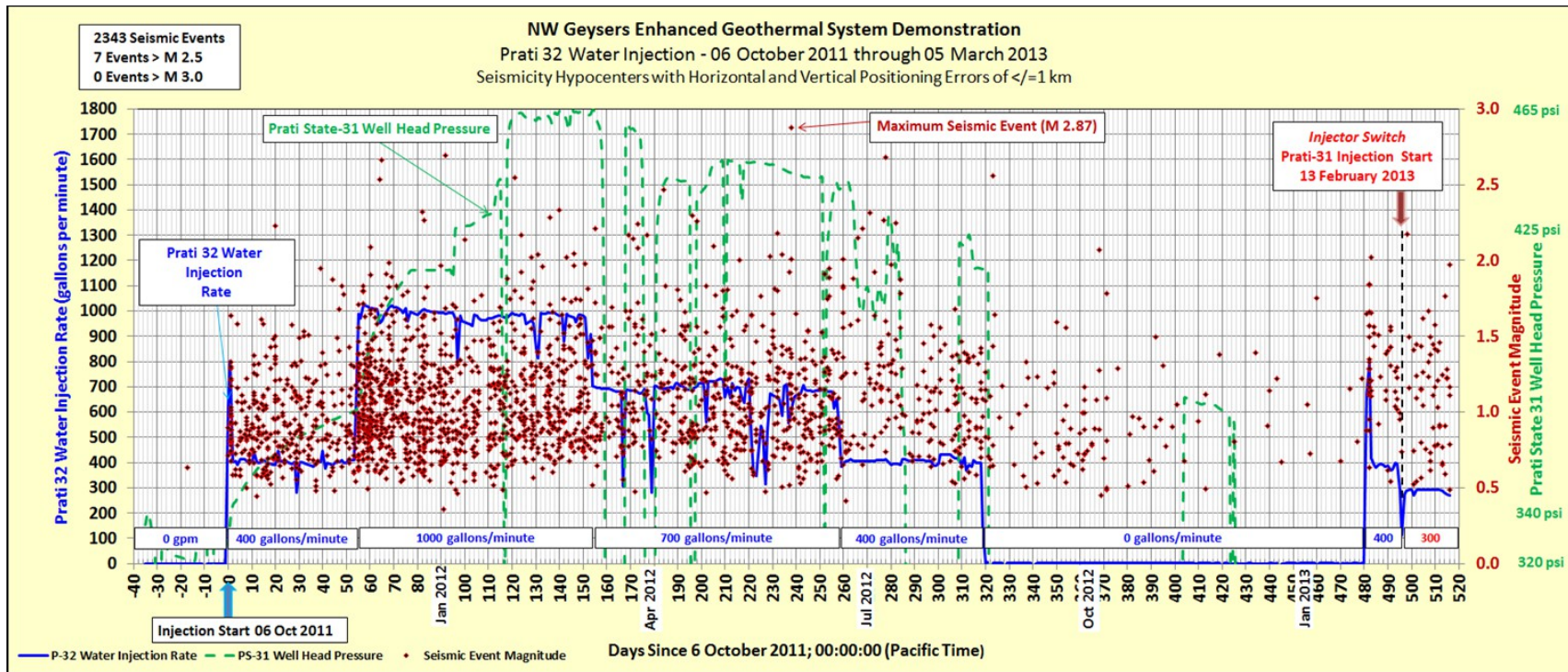
766  
768



769 Figure 18: The Geysers Production Areas, Power Plant Locations, Primary Inactive Fault Zones,  
770 Permanent Seismic Monitoring Networks and Temporary Seismic Monitoring Networks.

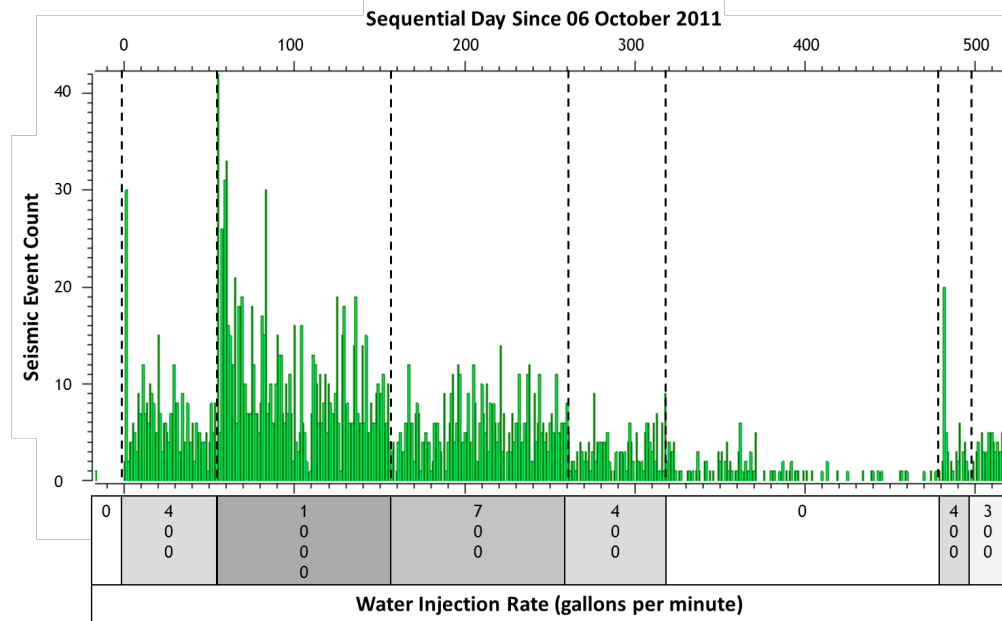


772 Figure 19: Map view of microseismic events from 01 September 2011 through 05 March 2013. The  
 773 microseismic events are diamonds with color and size scaled to event magnitude. The area of detailed  
 774 seismicity analysis is 3650 feet in the east-west dimension and 4860 feet in the north-south dimension  
 775 and defined as: Longitude 122.8459° W to 122.8333° W (California II 402 Easting 1759041 to  
 776 1762691) Latitude 38.8336° N to 38.8471° N (California II 402 Northing 426108 to 430968).



778 Figure 20: P-32 water injection (blue line and left axis), PS-31 well head pressure (green line and far right axis) and seismic event magnitude  
 779 (diamonds and near right axis) for the period from 40 days prior to injection through 520 days after injection initiation.

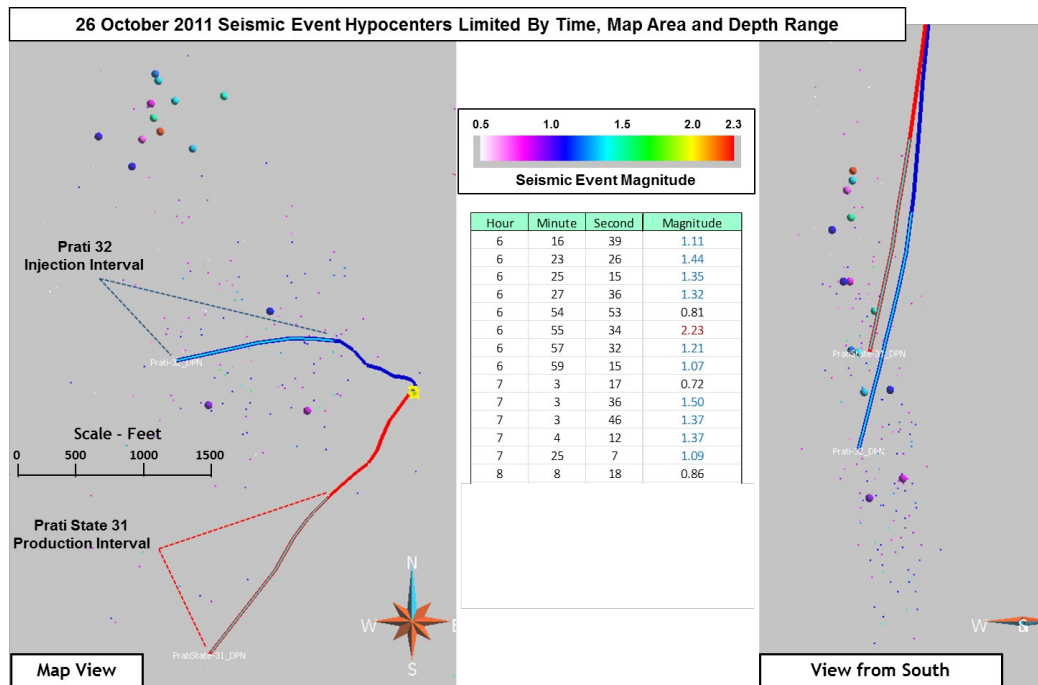
780



782

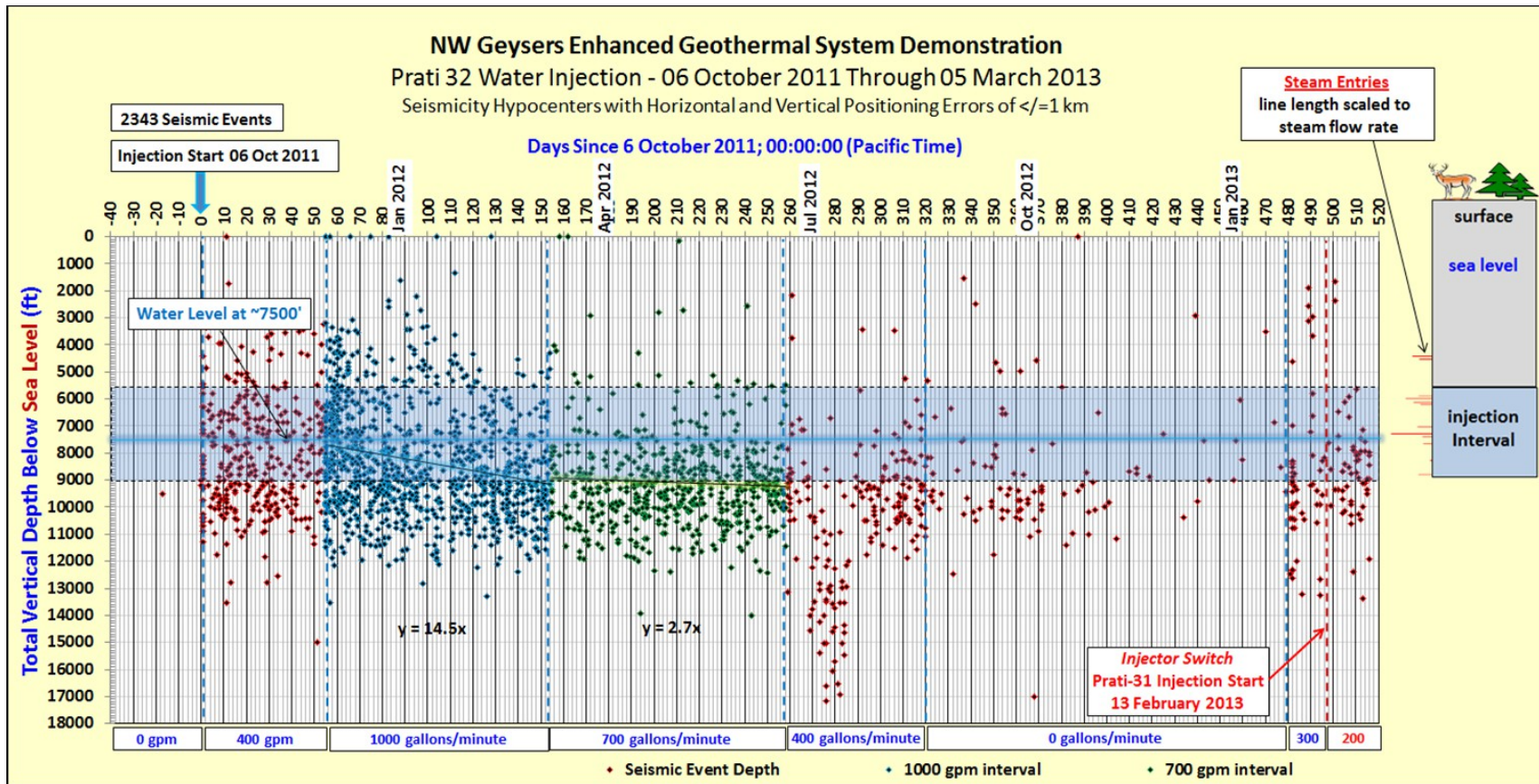
783 Figure 21: Water injection rate vs. seismic event count for the period from 40 days prior to start of  
784 injection on October 6, 2013 through 520 days after injection started.

785



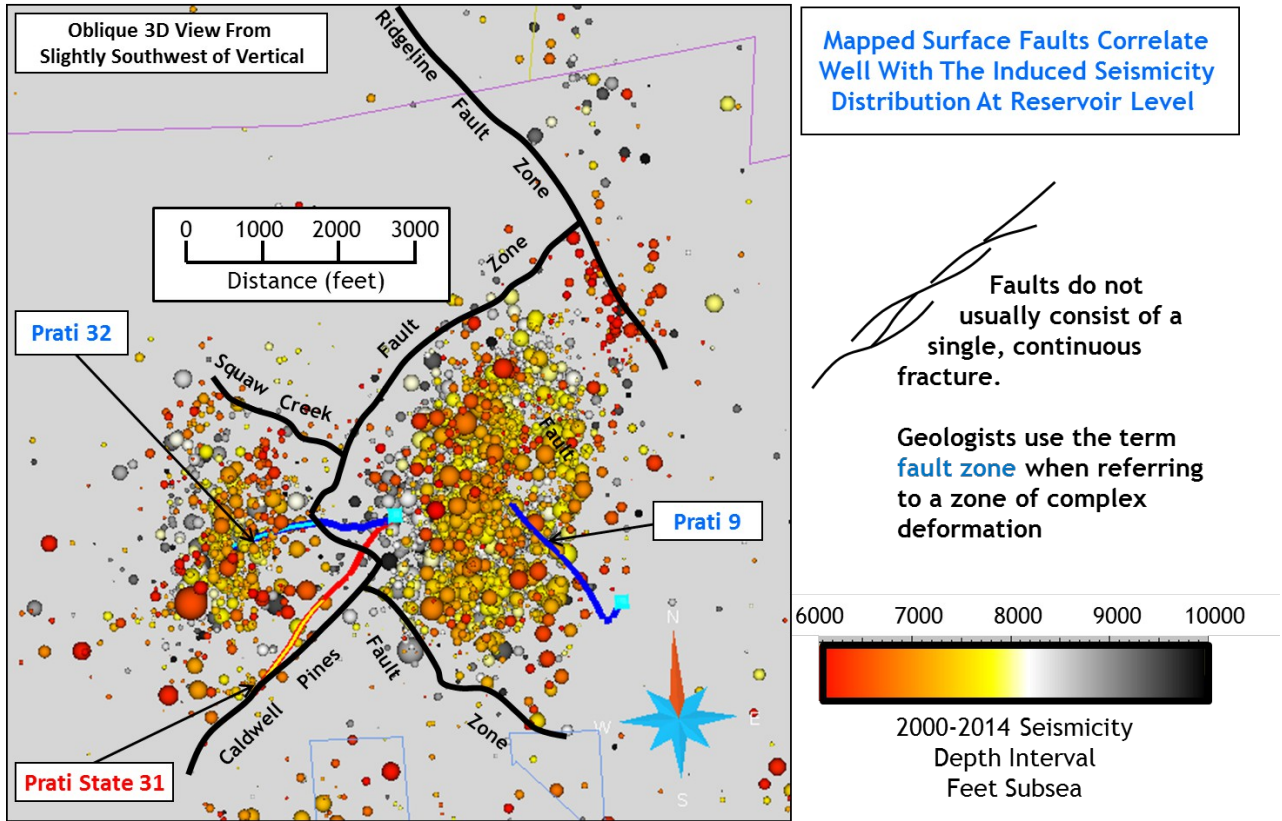
787 Figure 22: Map view (left) and cross sectional view from south (right) of the P-32 injector (blue), PS-  
788 78831 producer (red) and the seismicity hypocenters associated with a period of approximately two hours  
789 on 26 October 2011. Details concerning the seismic event timings and magnitudes are in the center of  
790 the display. This temporally and spatially limited seismicity cluster is believed to indicate fracture  
791 reactivation within a previously unaffected volume.



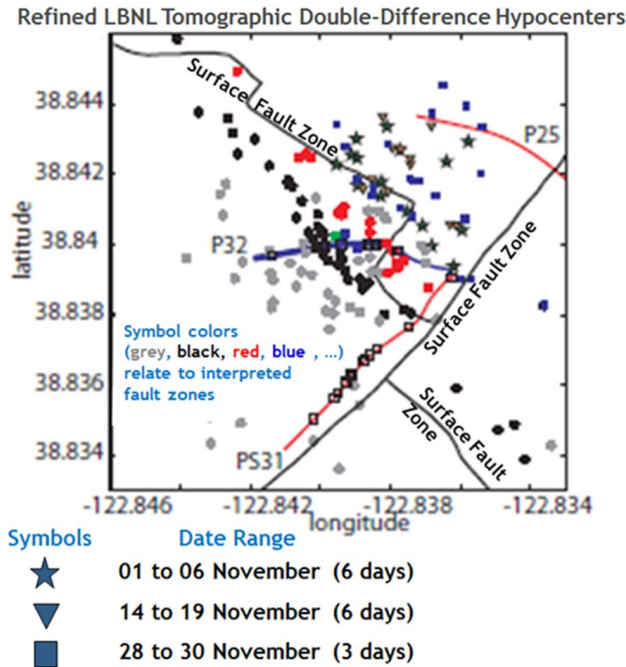


793Figure 23: Seismic event depth (diamonds) for the period from 40 days prior to injection through 520 days after injection initiation. The linear  
794least-squares fit is displayed for both the 1000 gpm injection interval ( $y = 14.5x$ ) and the 700 gpm injection interval ( $y = 2.7x$ ).

795  
796

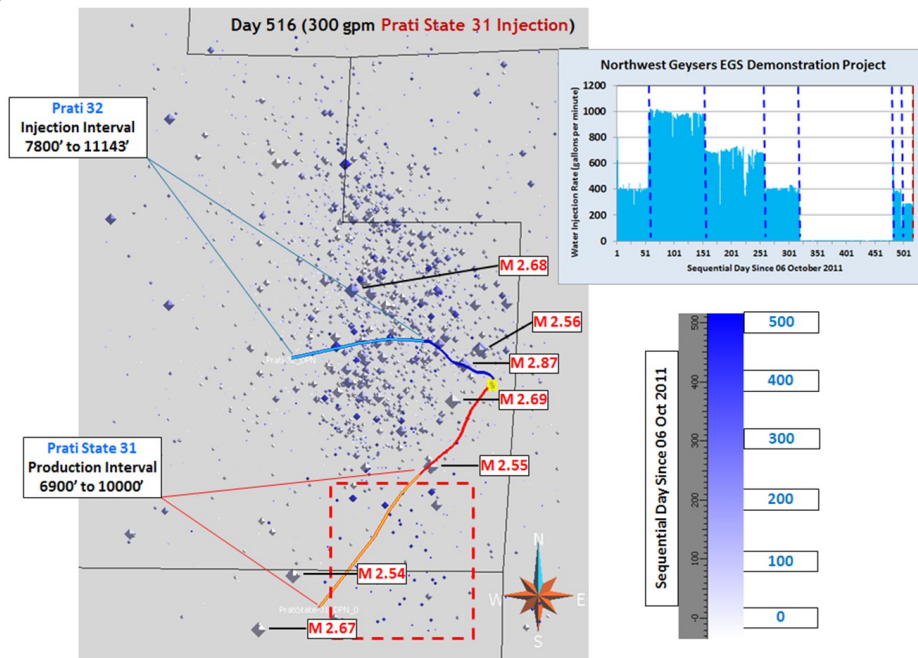


797Figure 24: Map view (right) and zoomed oblique view (left) of seismicity in the Northwest Geysers  
798and known surface fault zones (black solid and dashed lines). Recently noted linear seismicity  
799boundaries to the southeast and northeast of the P-32 injection well appear to be confined to the  
800northwest of the steeply northwest dipping Caldwell Pines Fault Zone and a steeply northeast dipping  
801Squaw Creek Fault Zone.



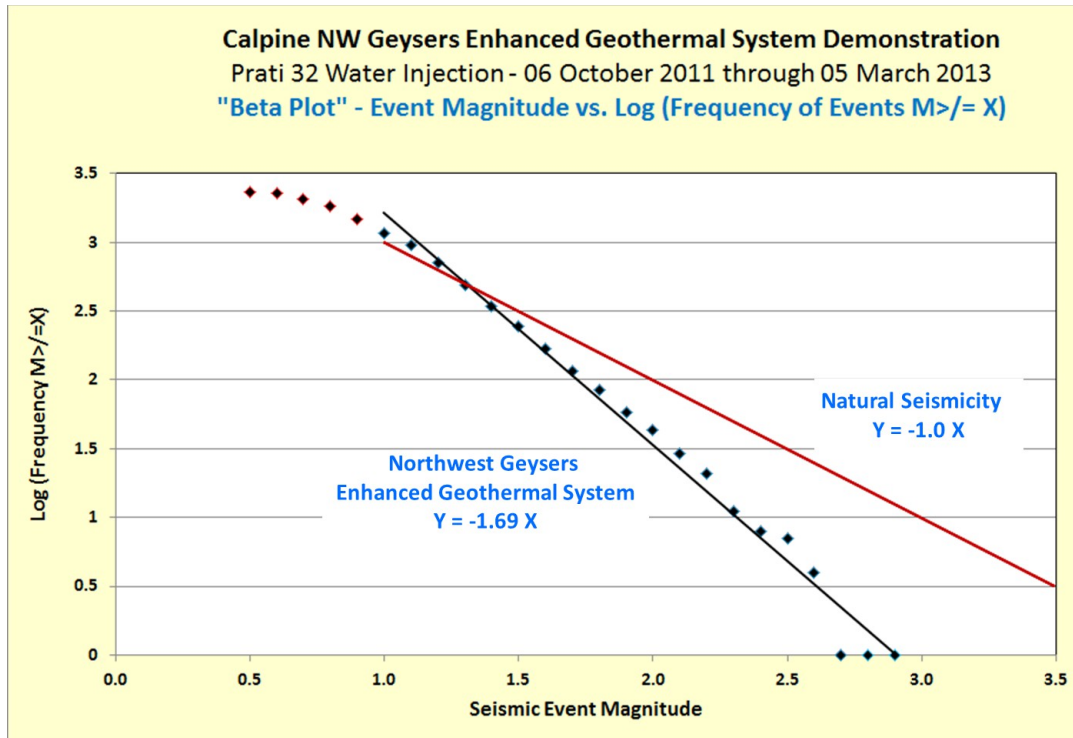
803 Figure 25: Map view of the relationship between previously mapped surface fault zones and  
 804 subsurface fault zones interpreted from seismicity hypocenters. Figure modified from Jeanne et al.  
 805 (2014b).

806



808 Figure 26: Map view of microseismic events from 01 September 2011 through 05 March 2013. The  
 809 microseismic events are displayed as diamonds with their size scaled to event magnitude and color  
 810 scaled to the sequential day since injection started (scale at lower right). The recent dark blue events  
 811 within the red dashed box occurred after the transition from 400 gpm water injection at P-32 to 300  
 812 gpm water injection at PS-31.

813



814

815 Figure 27: Gutenberg-Richter relationship between the magnitude  $x$  of a seismic event and the total  
816 number of seismic events with magnitudes higher than  $x$ . This generally expressed as  $\log N(x) = a -$   
817  $b \cdot x$ .

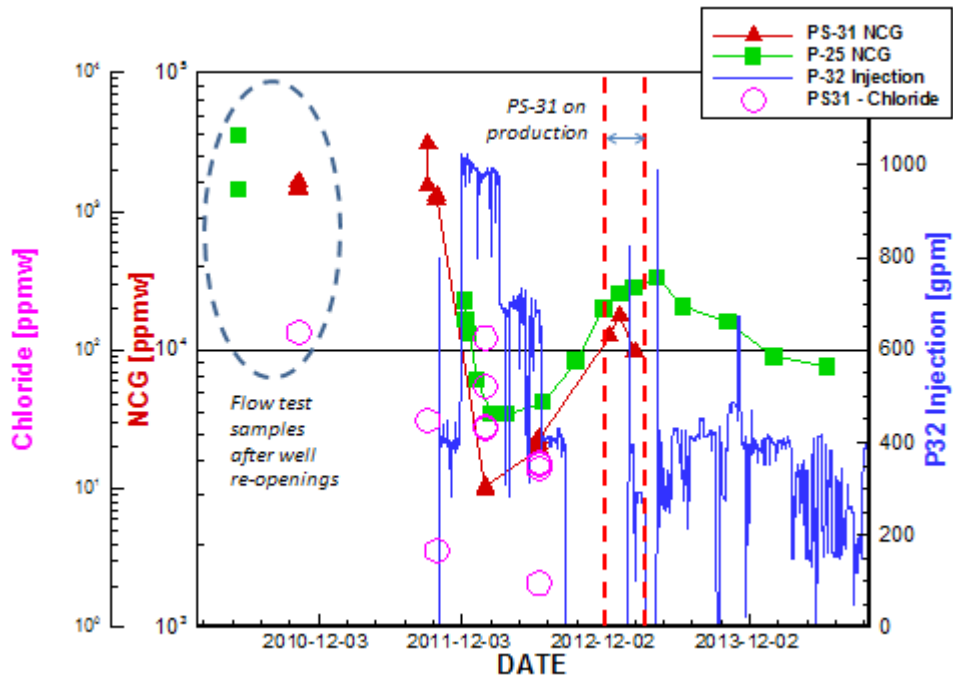
818

819

820

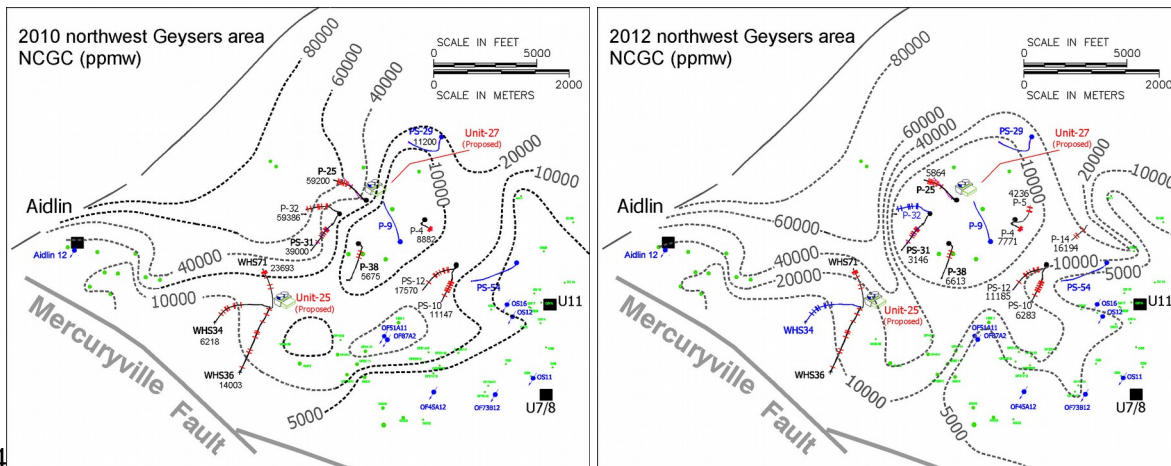


821



822  
823

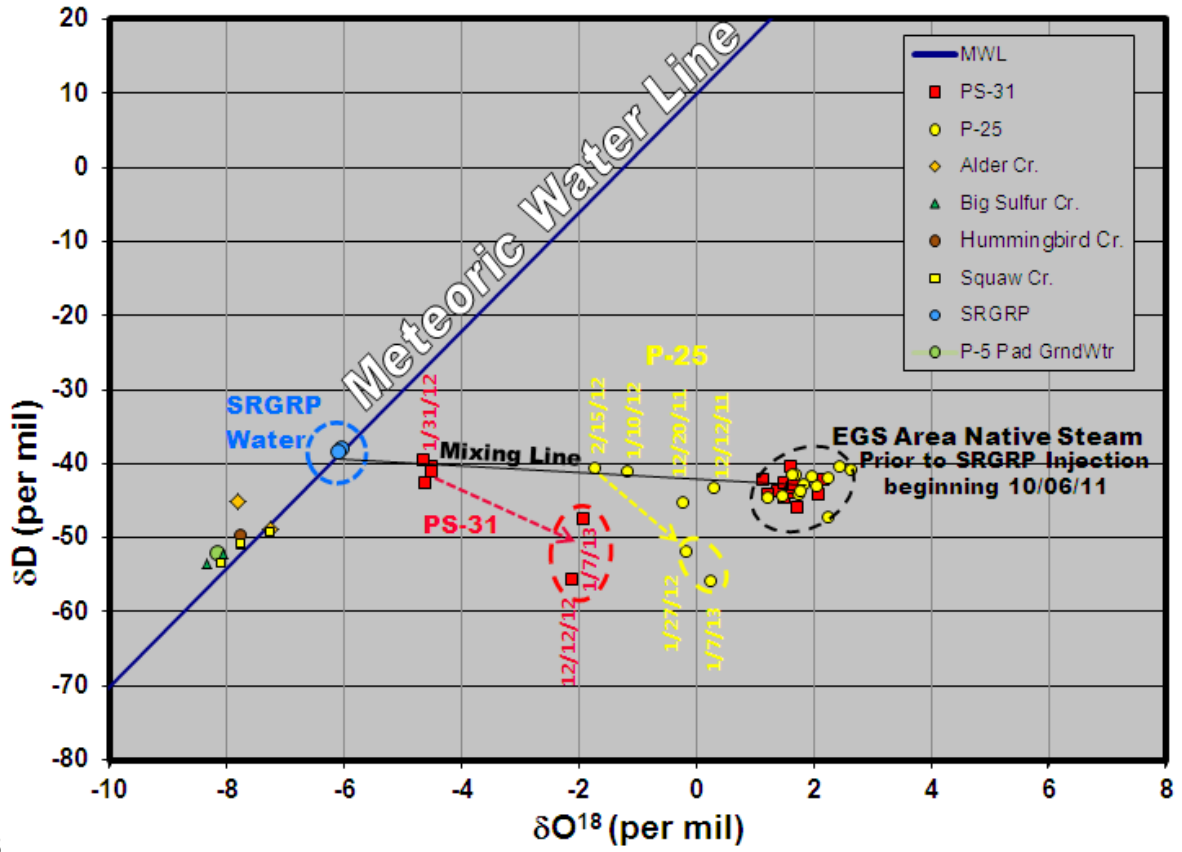
Figure 28: NCG and Chloride concentrations in PS-31 and P-25



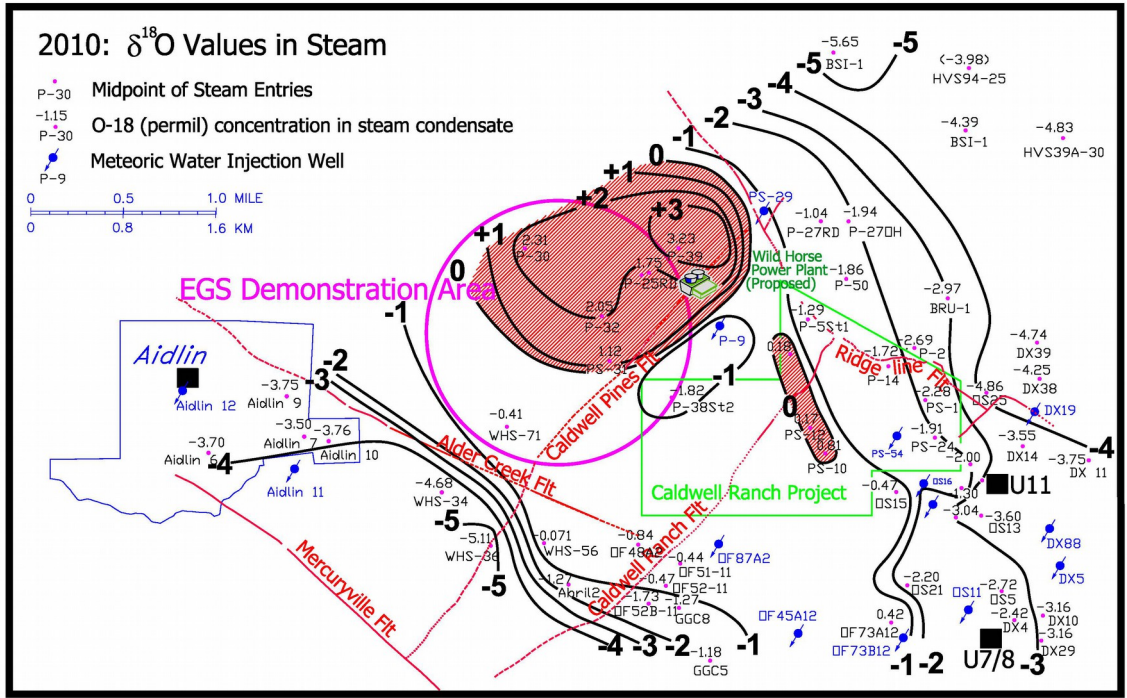
824

825 Figure 29: Northwest Geysers NCG concentrations before P-32 water injection (above) and 2  
826 months after the start of P-32 water injection (below)  
827

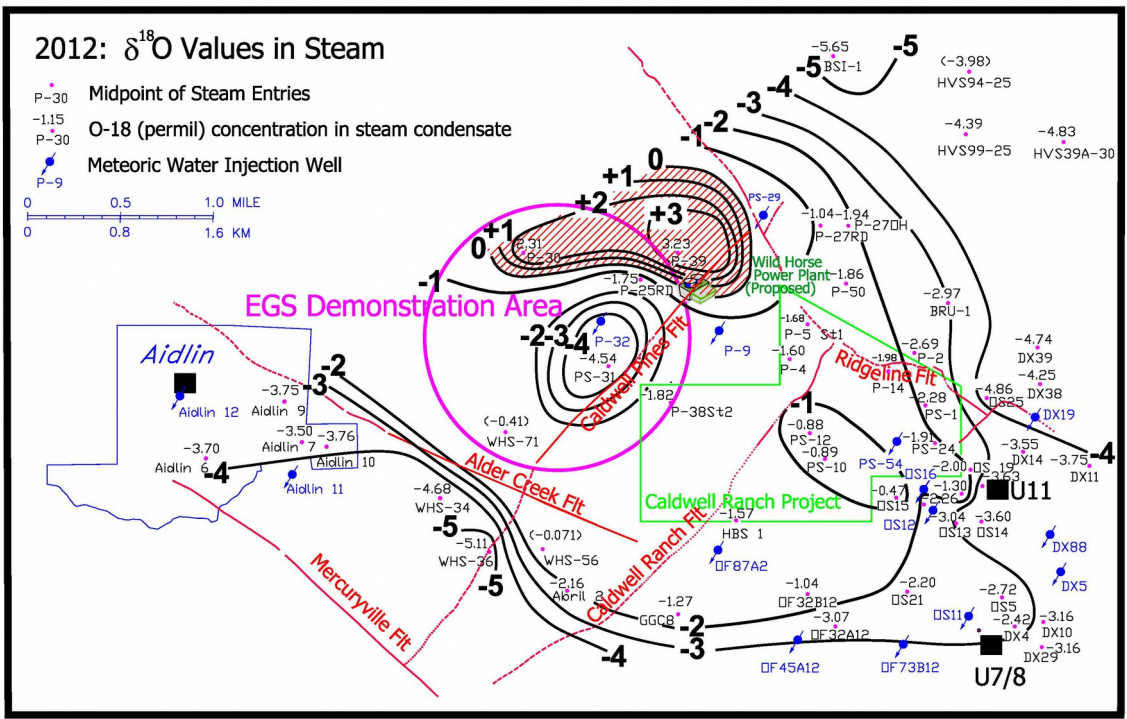
### Isotopic Mixing of SRGRP Water and Native Steam in PS-31



828  
 829 Figure 30: Changes to the isotopic composition of native steam by SRGRP water injection.  
 830  
 831



832



833  
834  
835  
836  
837  
838  
839

Figure 31: 2010-2011  $\delta^{18}\text{O}$  isotopic values in steam (top) and 2012  $\delta^{18}\text{O}$  isotopic values in steam (bottom)

840  
841  
842

Table 1. PS-31 well testing flow and geochemistry results

<b>PS-31</b>	<b>KPH</b>	<b>WHP</b>	<b>SIWHP</b>	<b>NCG</b>	<b>H<sub>2</sub>S</b>	<b>Cl</b>
<b>Orifice</b>	Testing	(klbs/hr)	(psig)	wt%	ppmw	ppmw
10/13/2010	42.9	100	320	4.5	1386	135
9/7/2011	52.7	100		4.7	1299	31
9/29/2011	52	100		3.5	1077	3.6
1/31/2012				0.32	545	27-123
6/14/2012				0.46	628	0.67-15.3
<b>Production</b>						
12/12/2012				1.1	767	13.5
1/7/2013				1.3	808	23
2/13/2013				0.98		

843  
844

## 845 REFERENCES

846

847 Aki, K. and Richards P.G. (1980), Quantitative Seismology: Theory and Methods, 932 pp, Freeman,  
848 San Francisco, CA.

849

850 Beall, J., Wrigth, M., and Hulen, J. (2007). Pre- and post-development influences on fieldwide  
851 Geysers NCG concentrations. In GRC Transactions, volume 31, pages 427-434.

852

853 Bertini, G., G. Gianelli, E. Pandeli, and M. Puxeddu, 1985, Distribution of hydrothermal minerals in  
854 Larderello-Travale and Mt. Amiata geothermal fields, Geotherm. Resour. Coun. Trans., v. 9,  
855 part 1, p. 261-266.

856

857 Boyle, K. and Zoback, M. (2014). The stress state of the Northwest Geysers, California geothermal  
858 field, and implications for fault-controlled fluid flow. Bulletin of the Seismological Society of  
859 America, 104(5).

860

861 DeCourten, F. (2008). Geology of Northern California. Available:

862 <[http://www.cengage.com/custom/regional\\_geology.bak/data/DeCourten\\_0495763829\\_LowRes\\_](http://www.cengage.com/custom/regional_geology.bak/data/DeCourten_0495763829_LowRes_New.pdf)  
863 [New.pdf](http://www.cengage.com/custom/regional_geology.bak/data/DeCourten_0495763829_LowRes_New.pdf)>. Accessed: July 21, 2015.

864

865 Drenick, A. (1986). Pressure-temperature-spinner survey in a well at The Geysers, Proceedings, 1 lth  
866 Workshop on Geothermal Reservoir Eng., Stanford, p. 197-205.

867

868 Garcia, J., Walters, M., Hartline, C., Pingol, A., Pistone, S., and Wright, M. (2012). Overview of the  
869 North-west Geysers EGS demonstration project. In Proceedings of the Thirty-Seventh Workshop  
870 on Geothermal Reservoir Engineering, Stanford University, volume 37.

871

872 Gutenberg, B. and Richter, C.F. (1942). Earthquake magnitude, intensity, energy and acceleration.  
873 Bull. Seismol. Soc. Am., 32: 163-191

874

875 Haizlip, J.R. (1985). Stable isotopic composition from wells in the northwest Geysers, Sonoma  
876 County, GRC Transactions, v.9, p. 133-138.

877

878 Hanks, T. and Kanamori H. (1979). A moment magnitude scale, *Journal of Geophysical Research*, 84,  
879 2348-2350.  
880

881 Jeanne, P., Rutqvist, J., Dobson, P., Walters, M., Hartline, C., and Garcia, J. (2014a). The impacts of  
882 mechanical stress transfers caused by hydromechanical and thermal processes on fault stability  
883 during hydraulic stimulation in a deep geothermal reservoir. *International Journal of Rock*  
884 *Mechanics and Mining Sciences*.  
885

886 Jeanne, P., Rutqvist, J., Hartline, C., Garcia, J., Dobson, P., and Walters, M. (2014b). Reservoir  
887 structure and properties from geomechanical modeling and microseismicity analyses associated  
888 with an enhanced geothermal system at The Geysers, California. *Geothermics*, 51:460-469.  
889

890 Kulhanek, O, 2005. Seminar on b-value, Department of Geophysics, Charles University, Prague  
891 (December 10-19, 2005) <http://geo.mff.cuni.cz/magma/magma-051214.pdf>  
892

893 Lockner, D. A., Summers, R., Moore, D., and Byerlee, J. D. (1982). Laboratory measurements of  
894 reservoir rock from The Geysers geothermal field, California. *Int. J. Rock Mech. Min. Sci. &*  
895 *Geomech*, 19:65-80.  
896

897 Lowenstern, J.B. and Janik, C.J., 2003. The origins of reservoir liquids and vapors from The Geysers  
898 geothermal field, CA. *Society of Economic Geologists, Special Publication 10*, p. 181-195.  
899

900 Lutz, S., Walters, M., and Moore, J. (2012). New insights into high-temperature reservoir, Northwest  
901 Geysers. In *GRC Transactions*, volume 36, pages 907-916.  
902

903 Moore, J.N., Norman, D.I. and Kennedy, M. (2001). Fluid inclusion gas compositions from an active  
904 magmatic-hydrothermal system: A case Study of The Geysers geothermal field, USA: *Chemical*  
905 *Geology*, v.173, p.3-30.  
906

907 Moore, J. and Gunderson, R. (1995). Fluid inclusion and isotopic systematics of an evolving magmatic  
908 hydrothermal system. *Geochimica et Cosmochimica Acta*, 59(19):3887-3907.  
909

910 Nielson, D. and Moore J. (2000). The Deeper Parts of The Geysers Thermal System - Implications  
911 For Heat Recovery. In *GRC Transactions*, volume 24, pages 299-302.  
912

913 Nielson, D., Walters, M., and Hulen, J. (1991). Fracturing in the Northwest Geysers, Sonoma County,  
914 California. In *GRC Transactions*, volume 15, pages 27-33.  
915

916 Oppenheimer, D. (1986). Extensional tectonics at The Geysers geothermal area, California.  
917 *Geophysical Research*, 91:11463-11476.  
918

919 Pruess K., Spycher N., and Kneafsey, T. J. (2007). Water Injection as a means for reducing non-  
920 condensable and corrosive gases in steam produced from vapor-dominated reservoirs, *Proceedings*,  
921 *Thirty-Second Workshop on Geothermal Reservoir Engineering Stanford University, Stanford*,  
922 *California, January 22-24, 2007*.  
923

924 Pruess, K., Celati, R., Calore, C., and Cappetti, G. (1987). On fluid and heat transfer in deep zones of \  
925 vapor dominated geothermal reservoirs, *Proceedings 12th Workshop Geothermal Reservoir Eng.*,  
926 *Stanford, CA*.  
927

928Rutqvist, J., Dobson, P., Garcia, J., Hartline, C., Hutchings, L., Jeanne, P., Oldenburg, C., Singh, A.,  
929 Vasco, D., and Walters, M. (2015a). The Northwest Geysers EGS demonstration project,  
930 California: Part 2: Modeling and interpretation. *Geothermics*, this issue.  
931

932Rutqvist, J., Dobson, P., Garcia, J., Hartline, C., Jeanne, P., Oldenburg, C., Vasco, D., and Walters, M.  
933 (2015b). The Northwest Geysers EGS demonstration project, California: Pre-stimulation modeling  
934 and interpretation of the stimulation. *Mathematical Geology*, 47:3-26.  
935

936Rutqvist, J., Dobson, P., Oldenburg, C., Garcia, J., and Walters, M. (2010). The Northwest Geysers  
937 EGS demonstration project phase 1: Pre-stimulation coupled geomechanical modeling to guide  
938 stimulation and monitoring plans. In *GRC Transactions*, volume 34, pages 1243-1250.  
939

940Segall, P. and Fitzgerald S.D. (1998). A note on induced stress changes in hydrothermal and  
941 geothermal reservoirs, *Tectonophysics*, 289(1-3) 117-128, doi:10.1016/S0040-1951(97)00311-9.  
942

943Stark, M. (2003). Seismic Evidence for a Long-lived Enhanced Geothermal System (EGS) in the  
944 Northern Geysers Reservoir, *GRC Transactions*, volume 27, pages 727-731  
945

946Shook, M. (1993). Numerical Investigations into the Formation of a 'High Temperature Reservoir,  
947 Proceedings, Eighteenth Workshop on Geothermal Reservoir Engineering, Stanford University,  
948 Stanford, California, January 26-28, 1993  
949

950Tester, J., Anderson, B., Batchelor, A., Blackwell, D., DiPippo, R., and Drake, E. (2006). The future of  
951 geothermal energy. part 1: Summary and part 2: Full report, massachusetts institute of technology.  
952

953Truesdell A.H. (1991). The origin of high-temperature zones in vapor-dominated geothermal systems,  
954 Proceedings, Sixteenth Workshop on Geothermal Reservoir Engineering Stanford University.  
955 Stanford, California. January 23-25.  
956

957Truesdell, A.H., Kennedy, B.M., Walters, M., and D'Amore (1994). New evidence for a magmatic  
958 origin of some gases in The Geysers geothermal reservoir, Proceedings, Nineteenth Stanford  
959 Geothermal Workshop SGP-TR-147, p. 297-301.  
960

961Truesdell A.H. and Shook M.G. (1997). Effect of injection into the high-temperature reservoir of the  
962 NW Geysers – A cautionary tale. PROCEEDINGS, Twenty-Second Workshop on Geothermal  
963 Reservoir Engineering Stanford University, Stanford, California, January 27-29, 1997  
964

965Walters, M. and Beall, J. (2002). Influence of meteoric water flushing on the non-condensable gas and  
966 whole-rock isotope distributions in the Northwest Geysers. In *GRC Transactions*, volume 26.  
967

968Walters, M.A., Moore, J.N., Renner, J.L., Nash, G., 1996. Oxygen isotope systematics and reservoir  
969 evolution of the northwest Geysers, *GRC transactions*, v.20, pp. 413-421.  
970

971Walters, M., Haizlip, J., Sternfeld, J., Drenick, A., and Combs, J. (1992). A vapor-dominated high-  
972 temperature reservoir at The Geysers California. In *GRC Monograph on The Geysers geothermal*  
973 *field*, Special Report no 17, pages 77-87.  
974

975Walters, M.A., J.N. Sternfeld, J.R. Haizlip, A.F. Drenick, and J. Combs, 1988, A vapor-dominated  
976 reservoir exceeding 600 °F at The Geysers, Sonoma County, California, Proceedings 13th  
977 Workshop on Geothermal Reservoir Eng., Stanford, p. 73-81.  
978

979Williams, C., Galanis, S., Moses, T., and Grubb, F. (1993). Heat flow studies in the Northwest Geysers  
980 geothermal field. In GRC Transactions, volume 17.  
981  
982Zang, A, V. Oye, P. Jousset, N. Deichmann, R. Gritto, A. McGarr, E. Majer, D. Bruhn, 2014. Analysis  
983 of induced seismicity in geothermal reservoirs – An overview. Geothermics, Volume 52, October  
984 2014, Pages 6–21, <http://www.sciencedirect.com/science/article/pii/S0375650514000753>  
985  
986